tapraid3/zpt-pt/zpt-pt/zpt01211/zpt9629d11z | xppws | S=1 | 10/22/11 | 15:56 | 4/Color Figure(s): 6,8 | Art: 185348 | Input-KAF

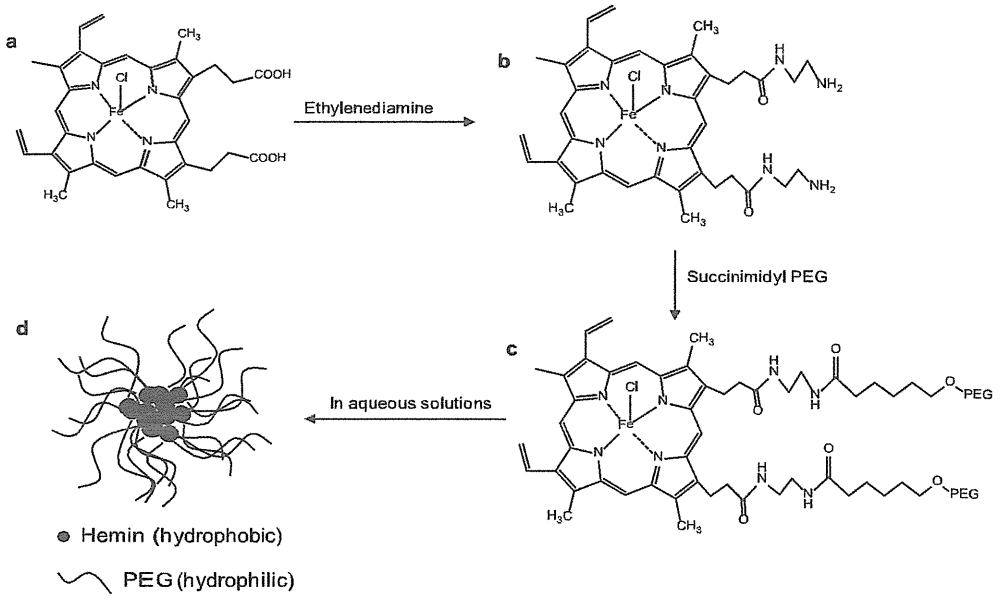

Scheme 1. Synthesis and chemical structure of PEG-hemin. a and b, an amino group was introduced into hemin (a; $C_{34}H_{32}ClFeN_4O_4$) by using ethylenediamine, which resulted in bis(ethylenediamino) hemin (b; $C_{38}H_{46}ClFeN_8O_2$), which was pegylated via succinimidyl PEG. c and d, the resultant PEG-hemin [c; $CH_3O(CH_2CH_2O)_n$-CO-$CH_2CH_2CH_2$-CO- $C_{38}H_{45}ClFeN_8O_2$] formed micelles (d) in aqueous solutions.

tervals, mice were killed and blood was collected in the presence of heparin, so that plasma could be obtained after centrifugation at 5000*g* for 20 min at 4°C. Then, 1.8 ml of ethanol with 0.25 M HCl was added to 0.2 ml of plasma to extract PEG-hemin or hemin. After vigorous vortexing and centrifugation at 20,000*g* for 20 min, supernatant UV spectra between 300 and 600 nm were measured, and peak absorbance at 385 nm was used to calculate the concentration of hemin according to the standard curve of hemin.

In Vitro Cytotoxicity Assay of PEG-Hemin. Human hepatocytes (Hc) were plated at 3000 cells/well in a 96-well plate (NUNC A/S, Roskilde, Denmark). After overnight preincubation, different concentrations of PEG-hemin were added to the cells. After an additional 48-h incubation, cell viability was determined by using the 3-(4,5-dimethylthiazol-2-yl)-2,5-diphenyltetrazolium bromide assay (Dojindo Laboratories, Kumamoto, Japan). AQ: H

Induction of HO-1 Expression in Human Hepatocytes by PEG-Hemin. To investigate the HO-1-inducing activity of PEG-hemin, HO-1 expression in human Hc was determined with or without PEG-hemin treatment. Hc cells were plated in six-well culture plates (50,000 cells/well), incubated overnight at 37°C, and treated with the indicated concentrations of PEG-hemin for 24 h. Cells were then collected, and total RNA and protein were extracted by using TRIzol reagent (Invitrogen, Carlsbad, CA) and CelLytic MT (Sigma-Aldrich) reagent, according to the manufacturers' instructions. Reverse transcription-PCR was performed for quantification of HO-1 copies in Hc cells. Primers used for PCR were as follows: HO-1 antisense 21-mer, 5′-GATGTTGAGCAGGAACGCGAT-3′, and HO-1 sense 21-mer, 5′-CAGGCAGAGAATGCTGAGTTC-3′, to obtain a 555-bp HO-1 cDNA (nucleotides 79–633); and GAPDH antisense 24-mer, 5′-CATGTGGGCCATGAGGTCCACCAC-3′, and sense 26-mer, 5′-TGAAGGTCGGAGTCAACGGATTTGGT-3′, to obtain a 983-bp GAPDH cDNA fragment. After an initial denaturing step at 94°C, 25 PCR cycles (30 cycles for GAPDH) were performed as follows: denaturing for 1 min at 94°C, primer annealing for 1 min at 56°C, and DNA synthesis for 1 min at 72°C. PCR products then underwent electrophoresis on ethidium bromide-stained 1% agarose gels. AQ: I

Experimental Protocol for Hepatic I/R Injury. Rats were fasted overnight before the experiment but were allowed free access to water. Animals were anesthetized with isoflurane during the operation by using an anesthesia system (SF-B01; DS Pharma Biomedical Co. Ltd). After the abdomen was shaved and disinfected with 70% ethanol, a complete midline incision was performed. The portal vein and hepatic artery were exposed and cross-clamped for 30 min with a noncrushing microvascular clip. Subsequently, reperfusion was initiated by removing the clips, and the abdomen was closed in two layers with 2-0 silk. Rats were kept warmed until they awoke and became active. Two hours before surgery for I/R, saline or PEG-hemin at different doses (2 or 10 mg/kg) was injected into each rat via the tail vein. In some experiments, a polymeric micellar HO-1 inhibitor, ZnPP, encapsulated with styrene maleic acid (SMA) copolymer, namely SMA-ZnPP (Iyer et al., 2007), was administered intravenously (5 mg/kg) just before I/R.

Measurement of Liver Enzyme Activity in Serum. Three hours after reperfusion resumed, rats were killed under anesthesia, and whole blood was withdrawn from the inferior vena cava. Activities of alanine aminotransferase (ALT), aspartate aminotransferase (AST), and lactate dehydrogenase (LDH) in serum were determined by means of the AutoAnalyzer system (Hitachi Ltd., Tokyo, Japan). Activities were expressed as IU/l.

Measurement of HO-1 Expression and Activity in Rat Liver after I/R. Liver tissues collected from rats receiving the above-described treatment with PEG-hemin or no treatment were homogenized with a Polytron homogenizer (Kinematica, Littau-Lucerne, Switzerland) in ice-cold homogenizing buffer (20 mM potassium phosphate buffer, pH 7.4, plus 250 mM sucrose, 2 mM EDTA, 2 mM phenylmethylsulfonyl fluoride, and 10 μg/ml leupeptin). Homogenates were centrifuged at 10,000*g* for 30 min at 4°C, and the resultant supernatant was ultracentrifuged at 105,000*g* for 1 h at 4°C. The microsomal fraction in the precipitates was suspended in 0.1 M potassium phosphate buffer, pH 7.4, followed by sonication for 2 s at 4°C.

Supernatant of the 10,000*g* fraction, with 50 μg of protein in each sample, was used for analysis of HO-1 expression by Western blot. In brief, total protein was separated by electrophoresis with 12% SDS-polyacrylamide gels and transferred to Immobilon polyvinylidene difluoride membranes (Millipore Corporation, Billerica, MA). This process was followed by reaction with a monoclonal antibody for HO-1 (GTS-1; Takara Bio Inc., Otsu, Shiga, Japan). The protein band that reacted immunologically with the antibodies was visualized by using the enhanced chemiluminescence system (GE Healthcare). AQ: J

The microsomal fraction was used for measurement of HO-1 activity. The HO reaction mixture consisted of the microsomal fraction (1 mg of protein), cytosolic fraction (supernatant after ultracentrifugation described above) of rat liver (1 mg of protein) as a source of biliverdin reductase, 33 μM hemin, and 333 μM NADPH in 1 ml of 0.1 M potassium phosphate buffer, pH 7.4. The mixture was incubated for 15 min at 37°C, after which the reaction was terminated by addition of 33 μl of 0.01 M HCl. Bilirubin formed in the reaction was extracted with 1.0 ml of chloroform, and bilirubin concentration was

determined spectroscopically by measuring the difference in absorbance between 465 nm (absorbance of bilirubin) and 530 nm (background), with a molar extinction coefficient of 40 $mM^{-1} \cdot cm^{-1}$ at 465 nm.

Moreover, HO-2 expression in this experimental protocol was measured by reverse transcription-PCR. In brief, total RNA of each liver tissue was extracted by using TRIzol reagent (Invitrogen) according to the manufacturers' instructions. Primers used for PCR were as follows: antisense, 5′-AGTAAAGTGCAGTGGTGGCC3-′, and sense, 5′-CAGCAACAATGTCTTCAGAGG-3′ to obtain a 230-bp HO-2 cDNA. After an initial denaturing step at 94°C, 35 PCR cycles were performed as follows: denaturing for 2 min at 92°C, primer annealing for 1 min at 54°C, and DNA synthesis for 1 min at 72°C. PCR products then underwent electrophoresis on ethidium bromide-stained 1% agarose gels.

Quantification of CO in Blood. After the I/R procedure just described, rats were killed and blood was collected. Each 0.35-ml sample of blood was diluted with 3.65 ml of phosphate-buffered saline and placed in a 10-ml glass test tube on ice. The test tubes were then sealed, and the air in the tubes was replaced by purging nitrogen gas into the tubes, after which the NO donor 3-(2-hydroxy-1-methyl-2-nitrosohydrazino)-*N*-methyl-1-propanamine was added, to a final concentration of 1 mM. Because NO has a much higher affinity than CO for hemoglobin, CO bound to hemoglobin would be liberated. After 2 h of incubation at room temperature, 1 ml of the gas in the test tubes was collected and processed in a gas chromatography CO analyzer (TRIlyzer mBA-3000; TAIYO Instruments, Inc., Osaka, Japan) equipped with a semiconductor gas sensor.

Preparation of Liver Tissue Sections for Histological Examination and Detection of Apoptosis. Rat livers were collected 3 h after I/R and cut into small tissue blocks (approximately 3–5 mm in length, width, and height). After the blocks were fixed with 6% buffered neutral formalin solution, they were embedded in paraffin. Paraffin-embedded sections (6 μm thick) were prepared as usual for histological examination after hematoxylin and eosin staining and for apoptosis staining (TUNEL) as described below.

In Situ Detection of Apoptosis in the Liver. TUNEL staining was used to investigate apoptosis in the paraffin-embedded sections described above, after I/R with or without PEG-hemin treatment, with an in situ apoptosis detection kit (TACS; Trevigen, Gaithersburg, MD), according to the manufacturer's instructions. TUNEL-positive cells in four different fields per sample were counted, and results were expressed per mm^2 of tissue section.

Detection of Caspase 3/7 Activities in the Liver. Apoptosis in the livers of different treatment groups were further examined in their caspase 3/7 activities, with a caspase assay kit that contains the substrate peptide DEVD (Caspase-Glo 3/7 Assay; Promega, Madison, WI). In brief, the liver tissue homogenates were prepared by using 1 g of wet tissue added with 4 ml of hypotonic extraction buffer (25 mM HEPES buffer, pH 7.5, 5 mM $MgCl_2$, 1 mM EGTA, 2 mM phenylmethylsulfonyl fluoride, and 10 μg/ml leupeptin) with the Polytron homogenizer (Kinematica). Homogenates were centrifuged at 10,000*g* for 30 min at 4°C, and the supernatant was used for caspase activity assay according to the manufacturer's instructions.

Measurement of Liver Tissue Blood Flow. A laser Doppler flowmeter (ALF21; Advance Co. Ltd., Tokyo, Japan) was used to measure liver tissue blood flow in anesthetized animals during I/R (until 1 h after initiating reperfusion) with or without PEG-hemin treatment (10 mg/kg i.v.). The flowmeter probe was inserted at the same site in the median lobe of the liver in each animal. The real-time change in blood flow was monitored, and the mean blood flow at specific time points was calculated and expressed as a percentage of the preischemic initial blood flow value as the control.

Thiobarbituric Acid-Reactive Substance Assay. Oxidative cell damage in the liver after I/R with or without PEG-hemin treatment was quantified by assay of lipid peroxide formation via the thiobarbituric acid reaction (Ohkawa et al., 1979). In brief, liver tissue homogenates were prepared at a ratio of 1 g of wet tissue to 9 ml of 1.15% KCl in a Polytron homogenizer. Then, 0.1 ml of homogenate was mixed with 0.2 ml of 8.1% SDS, 1.5 ml of 20% acetic acid (pH 3.5 adjusted with NaOH), and 1.5 ml of a 0.8% aqueous solution of thiobarbituric acid. The final sample was made up to 4 ml with distilled water and incubated at 95°C for 60 min. After cooling with tap water, 1.0 ml of distilled water and 5.0 ml of a mixture of *n*-butanol and pyridine (15:1, v/v) were added, and each reaction mixture was shaken vigorously. After centrifugation at 5000*g* for 10 min, absorbance of the organic upper layer was measured at 532 nm.

ELISA for 8-Hydroxydeoxyguanosine in the Liver. Oxidative injury of the liver after I/R with or without PEG-hemin treatment was further examined by detecting 8-hydroxydeoxyguanosine (8-OHdG) in liver tissues, by use of an ELISA kit (8-OHdG Check; JalCA, Fukuroi, Shizuoka, Japan). In brief, DNA in each sample was extracted by using a QuickGene DNA tissue kit (DT-S; Wako Pure Chemicals), followed by hydrolysis using an 8-OHdG Assay Preparation Reagent Set (Wako Pure Chemicals). The ELISA was then performed to detect 8-OHdG according to the manufacturer's instructions.

ELISA for Monocyte Chemotactic Protein 1 in Serum. Serum samples from I/R-treated rats were obtained as described above, and the monocyte chemotactic protein 1 (MCP-1) levels were quantified by using an ELISA kit (Immuno-Biological Laboratories Co., Ltd., Takasaki-Shi, Gunma, Japan) according to the manufacturer's instructions.

Statistical Analysis. All data are expressed as means ± S.E. Student's *t* test was used to determine the significance between each experimental group. A difference was considered statistically significant when $P < 0.05$.

Results

Synthesis of PEG-Hemin. As we reported previously, to facilitate conjugation of hemin with PEG we first conjugated with ethytlenediamine to generate amino groups onto two carboxyl groups in the porphyrin ring of hemin, to produce more reactive nucleophiles than the original carboxyl group (Sahoo et al., 2002). Then, pegylation targeted to the amino groups was successfully achieved by using succinimidyl-activated PEG, with two PEG chains conjugated to the porphyrin structure of hemin (Scheme 1). The resulting PEG-hemin exhibited a high water solubility, more than 15 mM, whereas native hemin is almost insoluble in water or physiological solutions. Physiochemical analysis showed that PEG-hemin had a UV spectrum that was similar to that of free hemin (data not shown). IR spectra of PEG-hemin exhibited a characteristic absorption of amide bonds at 1654 cm^{-1} (amide I) and 1542 cm^{-1} (amide II) (Fig. 1), which demonstrated conjugation between PEG and hemin via amide bonds. Cross-link of PEG was further supported by the fact that PEG-hemin had no free amino groups after pegylation (Scheme 1), as determined by fluorescamine (data not shown). F1, AQ:K

The molecular mass of PEG-hemin, as calculated from the chemical structure of PEG-hemin shown in Scheme 1, was 10 to 12 kDa with two PEG molecules (approximately 5000 Da each) conjugated per mole of hemin. However, in aqueous solutions, PEG-hemin had a large molecular mass, approximately 126 kDa as analyzed by Sephadex G-100 column chromatography (Fig. 2A). This result was confirmed by DLS, F2 which showed a mean particle size of 121.5 nm in deionized water (Fig. 2B). The particle size of PEG-hemin in water remained unchanged at 4°C for more than 1 month. These data clearly indicated the formation of stable micelles of PEG-hemin in aqueous solution, with the hydrophobic core assembly of hemin inside and the hydrophilic PEG outside (Scheme 1).

tapraid3/zpt-pt/zpt-pt/zpt01211/zpt9629d11z | xppws | S=1 | 10/22/11 | 15:56 | 4/Color Figure(s): 6,8 | Art: 185348 | Input-KAF

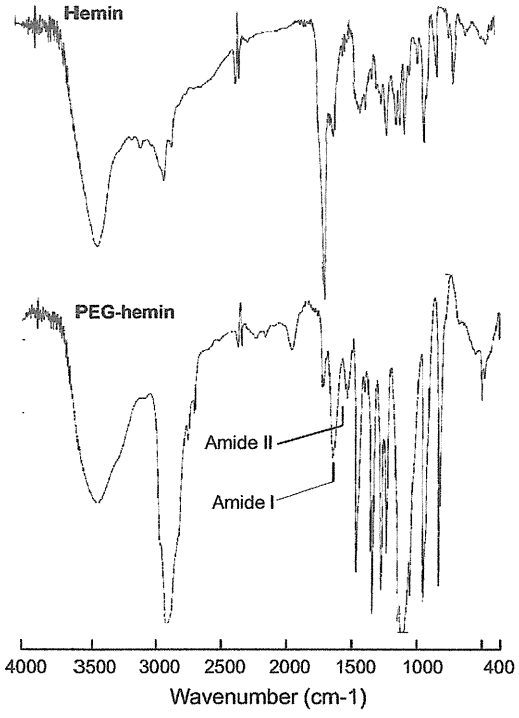

Fig. 1. IR spectra of hemin and PEG-hemin. Amide I (1654 cm^{-1}) and amide II (1542 cm^{-1}) were clearly observed in PEG-hemin, which suggested an amide bond formation between hemin and PEG through bis-(ethylenediamino) hemin.

Plasma $t_{1/2}$ of PEG-Hemin. We expected the macromolecular micellar formulation of PEG-hemin to have superior in vivo pharmacokinetics (e.g., prolonged $t_{1/2}$), and we investigated this possibility by using *ddY* mice. Compared with free hemin, PEG-hemin had a relatively long circulation time: even 20 h after intravenous injection, approximately 30% remained in circulation; almost no hemin was detected F3 2 h after administration (Fig. 3). The $t_{1/2}$ of PEG-hemin was calculated to be 18.2 h, which is approximately 20 times longer than that of hemin (0.96 h); in parallel, the AUC of PEG-hemin increased to 16 times of that of free hemin, and the total body clearance of PEG-hemin was approximately 16 T1 times slower than that of free hemin (Table 1).

In Vitro Cytotoxicity and HO-1 Induction Activity of PEG-Hemin. Figure 4A shows no apparent cytotoxicity for F4 PEG-hemin up to 250 μM (hemin equivalent). More important, PEG-hemin treatment significantly induced expression of HO-1 mRNA in cultured human hepatocytes (Fig. 4B).

In Vivo HO-1 Induction by PEG-Hemin in a Rat Liver I/R Model. The I/R procedure alone increased HO-1 protein expression in the liver tissue, but more important, this HO-1 expression was dramatically up-regulated by PEG-hemin treatment (Fig. 5A). Likewise, HO-1 activity in liver tissue, F5 as assessed by the production of bilirubin, increased after I/R but more significantly increased after I/R plus PEG-hemin treatment (Fig. 5B). These findings were supported by the PEG-hemin-induced significant increase in the blood concentration of CO, which is another major product of HO-1-catalyzed heme degradation (Fig. 5C).

In addition, I/R procedure induced a slight increase of HO-2 expression; however, PEG-hemin treatment did not affect HO-2 expression (Supplemental Fig. 1).

Amelioration of Liver I/R Injury by PEG-Hemin. The potential therapeutic or tissue protective effect of PEG-hemin against I/R injury of the liver was evaluated by measuring plasma concentrations of the liver enzymes AST, ALT, and LDH. In our previous study, we reported that these enzymes increased to a maximum level at 3 h after reperfusion (Ikebe et al., 2000); thus, in this study all experiments were performed at 3 h after reperfusion. As anticipated, I/R caused a large increase in the levels of all three liver enzymes, to more than 20 times of normal levels. AST, ALT, and LDH values for I/R versus those for normal rat were as follows: 2647.4 ± 460.4 IU/l versus 65.3 ± 0.7 IU/l, 1356.4 ± 182.1 IU/l versus 54.3 ± 1.2 IU/l, and 6932.6 ± 1131.0 IU/l versus 62.3 ± 3.4 IU/l, respectively) (Fig. 6A). F6

More important, PEG-hemin treatment, at 10 mg/kg (hemin equivalent), significantly lowered the elevated levels of AST, ALT, and LDH, with liver enzyme levels almost recovering to normal (Fig. 6A). Furthermore, this cytoprotective effect of PEG-hemin was almost nullified by administration of SMA-ZnPP, which is a macromolecular water-soluble HO inhibitor that we had prepared previously (Iyer et al., 2007) (Fig. 6A). These results suggest that the cytoprotective effect of PEG-hemin was through an HO-1-mediated pathway, as

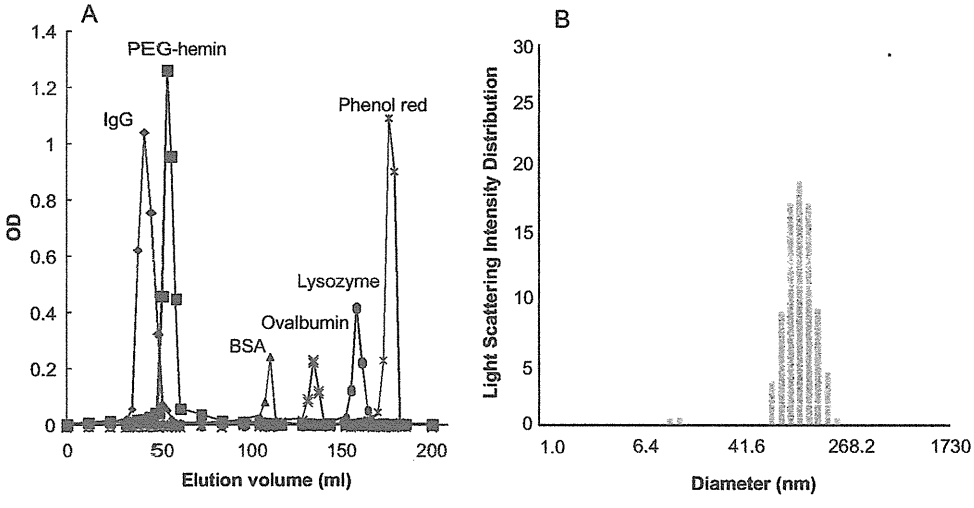

Fig. 2. Apparent molecular mass of PEG-hemin in aqueous solutions as analyzed by Sephadex G-100 gel chromatography (A) and DLS (B). Gel chromatography was performed with the mobile phase of 0.25 M $NaHCO_3$, pH 8.2, and the molecular mass of PEG-hemin in aqueous solutions was calculated by reference to known molecular mass protein markers. See *Synthesis of PEG-Hemin* under *Results* for details. BSA, bovine serum albumin.

AQ: O
AQ: P

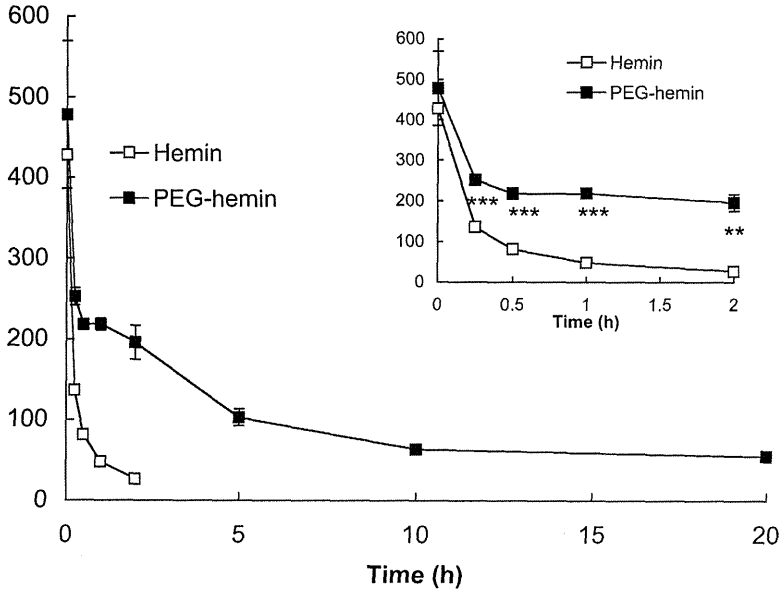

Fig. 3. Pharmacokinetics of PEG-hemin and native hemin in the blood of *ddY* mice. Native hemin or PEG-hemin was injected intravenously into *ddY* mice via the tail vein. After scheduled intervals, mice were killed, blood was collected, and blood concentrations of hemin and PEG-hemin were measured as described under *Materials and Methods*. Values are means ± S.E. ($n = 4$). **, $P < 0.01$; ***, $P < 0.001$, PEG-hemin versus native hemin.

TABLE 1

Pharmacokinetic parameters of free hemin and PEG-hemin

Plasma $t_{1/2}$ indicates time required to reach to half-concentration at time zero by interpolation.

Agent	$t_{1/2}$	AUC	Total Body Clearance
	h	*μg/ml/h*	*l/h/kg*
Hemin	0.96	203.3	49.2
PEG-hemin	18.25	3289.3	3.0

discussed in the *Introduction*. Consistent with these findings, hematoxylin and eosin staining of liver tissues after I/R revealed apparent necrotic areas, but necrosis was significantly inhibited by PEG-hemin treatment (Fig. 6B). In addition, rats not undergoing I/R showed no apparent changes in serum AST, ALT, and LDH values after injection of PEG-hemin (data not shown), which suggests that PEG-hemin seemed to be nontoxic to the liver.

Changes in Hepatic Blood Flow. One major reason for liver tissue injury by I/R is reduced blood flow, as clearly seen in Fig. 7, which shows that hepatic blood flow decreased to 20% of normal at 20 min after ischemia and recovered to only 30% of normal at 1 h after reperfusion was initiated. The tissue-protective effect of PEG-hemin was believed to result, at least in part, from improved hepatic blood flow. PEG-hemin treatment largely increased hepatic blood flow, which reached 80% of normal at 1 h after the start of reperfusion (Fig. 7).

Apoptosis in the Liver after I/R. The TUNEL assay for apoptosis allowed further elucidation of the pathological events caused by I/R with or without PEG-hemin treatment. I/R clearly induced apoptosis at 3 h after reperfusion, whereas PEG-hemin significantly lowered the number of apoptotic cells in the liver after I/R (Fig. 8A), findings that correlated well with the liver enzyme profiles. This was further supported by caspase 3/7 activity assay, by which the caspase 3/7 activities were found to be remarkably increased in the livers of I/R, whereas it was significantly inhibited by PEG-hemin (Fig. 8B).

Oxidative Injury Induced by I/R in the Liver. To investigate the role of ROS in liver I/R injury, the TBARS assay, which is a standard method of detecting oxidative injury of tissue involving lipid peroxidation, was performed. As Fig. 9 shows, I/R greatly increased the TBARS level in the rat liver. This increase was markedly inhibited by PEG-hemin treatment in a dose-dependent manner (Fig. 9): at 10 mg/kg PEG-hemin, the TBARS value was almost normal, which suggests that liver injury caused by I/R involved the increased generation of ROS. Similar results were obtained when 8-OHdG, which is a common index for oxidative injury of DNA, was detected in the liver of rat after I/R procedure with or without PEG-hemin treatment. These findings indicate the involvement of ROS in I/R injury and the protective effect of PEG-hemin in this process.

Change in Serum Inflammatory Cytokine MCP-1 Level after I/R With or Without PEG-Hemin. Inflammation is a major consequence of ROS-related diseases and thus plays a crucial role in the pathological process of I/R. Among the many inflammatory cytokines known to be involved in I/R injury, MCP-1, a proinflammatory chemokine and key mediator in the inflammatory process, is strongly associated with ROS-induced pathological conditions including I/R injury (Melgarejo et al., 2009). We thus measured the levels of MCP-1 in rat serum after I/R with or without PEG-hemin administration. Figure 10 shows a significantly increased serum MCP-1 level at 3 h after I/R. However, PEG-hemin treatment before I/R markedly inhibited this increase, which was consistent with the liver function results, as well as necrosis and apoptosis in liver tissue.

Discussion

During the past few decades, the clinical importance of ROS has been discussed extensively, and development of drugs to control the generation of ROS or scavenge ROS has become a focus of great interest (Maeda and Akaike, 1991; McCord, 2000). One approach is to block ROS generation. We in fact developed an XO inhibitor, 4-amino-6-hydroxypyrazolo[3,4-*d*]pyrimidine, and its polymer conjugate to inhibit O_2^- production by XO (Miyamoto et al., 1996; Fang et al., 2009a, 2010). An alternative approach that has attracted our

tapraid3/zpt-pt/zpt-pt/zpt01211/zpt9629d11z | xppws | S=1 | 10/22/11 | 15:56 | 4/Color Figure(s): 6,8 | Art: 185348 | Input-KAF

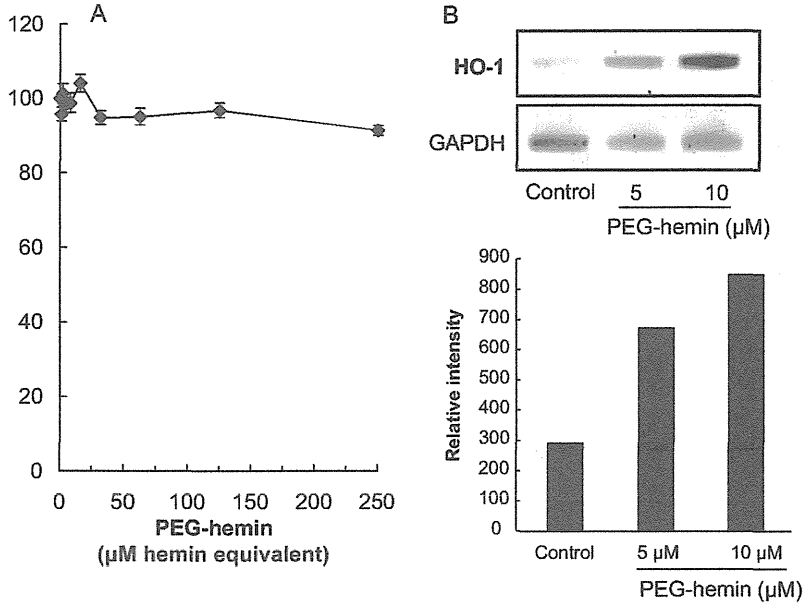

Fig. 4. In vitro cytotoxicity (A) and HO-1 induction activity (B) of PEG-hemin. The viability of human Hc was determined by using the 3-(4,5-dimethylthiazol-2-yl)-2,5-diphenyltetrazolium bromide assay. Values are means ± S.E. (n = 8 wells). See *In Vitro Cytotoxicity and HO-1 Induction Activity of PEG-Hemin* under *Results* for details.

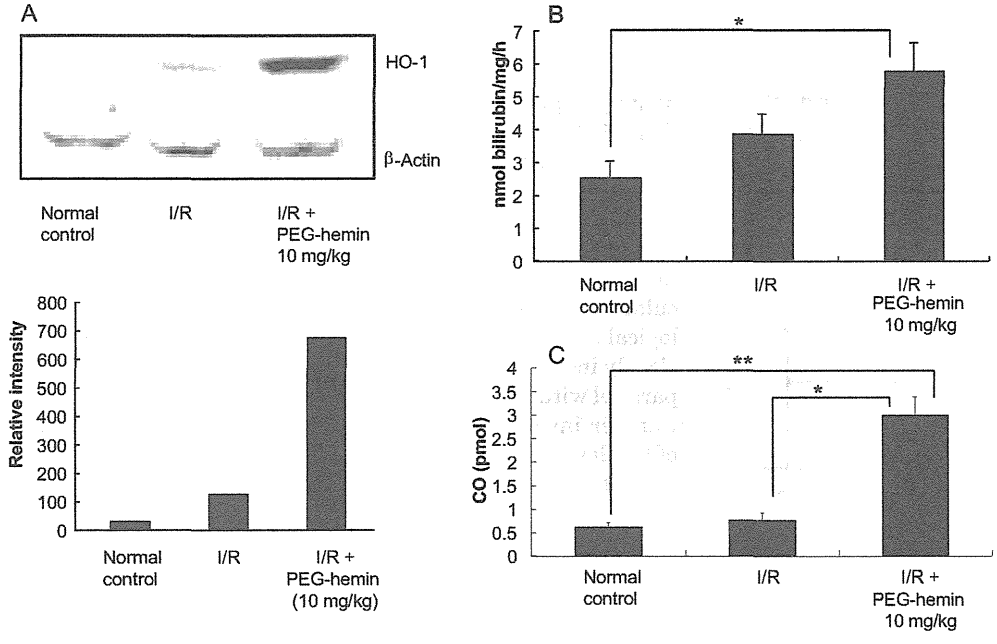

Fig. 5. In vivo induction of HO-1 by PEG-hemin in a rat I/R model. A and B, Western blot analysis for HO-1 protein in liver tissue (A) and HO-1 activity, as evidenced by bilirubin formation, in liver tissue after I/R with or without PEG-hemin treatment (B). C, HO-1 induction was further verified by measuring the CO concentration in blood. See *In Vivo HO-1 Induction by PEG-Hemin in a Rat Liver I/R Model* under *Results* for details. All data are presented as means ± S.E. (n = 4). *, $P < 0.05$; **, $P < 0.01$.

attention is to take advantage of the products of HO-1, which is a major antiapoptotic antioxidative molecule (Maines, 1988; Fang et al., 2004; Abraham and Kappas, 2008). Induction of HO-1 either by its inducers such as cobalt protoporphyrin and hemin or by HO-1 gene transfer showed beneficial effects in many ROS-related diseases (Fang et al., 2004; Abraham and Kappas, 2008). We followed this approach by using a modified hemin and developed a macromolecular micellar hemin formulation to improve its water solubility and in vivo pharmacokinetics.

We used PEG, which is a widely used biocompatible polymer, to prepare hemin micelles. Consistent with our previous reports of PEG-ZnPP (Sahoo et al., 2002; Fang et al., 2003), which is chemically similar to PEG-hemin, PEG modification of hemin led to markedly increased solubility (more than 15 mM; hemin equivalent) in physiological solutions, in which free hemin can be hardly solubilized. More important, PEG-hemin exhibited a very long circulation time: its $t_{1/2}$ in *ddY* mice was approximately 18 h, which was approximately 20 times longer than that of free hemin (Fig. 3; Table 1). Furthermore, PEG-hemin had no or very little toxicity; PEG-hemin treatment, up to 250 μM, produced no cell death (Fig. 4A). Its safety was also verified in vivo: injection of 100 mg/kg i.v. PEG-hemin into *ddY* mice did not cause the death of the mice or any apparent side effects such as loss of body weight and change in blood biochemistry (data not shown). These findings warrant further clinical applications of PEG-hemin.

The improved water solubility and plasma $t_{1/2}$ are caused by the micellar formulation of PEG-hemin, which had an apparent molecular mass of 126 kDa in aqueous solution as judged by Sephadex G-100 column chromatography (Fig. 2A). This PEG-hemin presents as an aggregated micellar form, as observed by DLS, which showed a mean particle size of 121.5 nm in physiological solution (Fig. 2B). Macromolecular drugs

COLOR

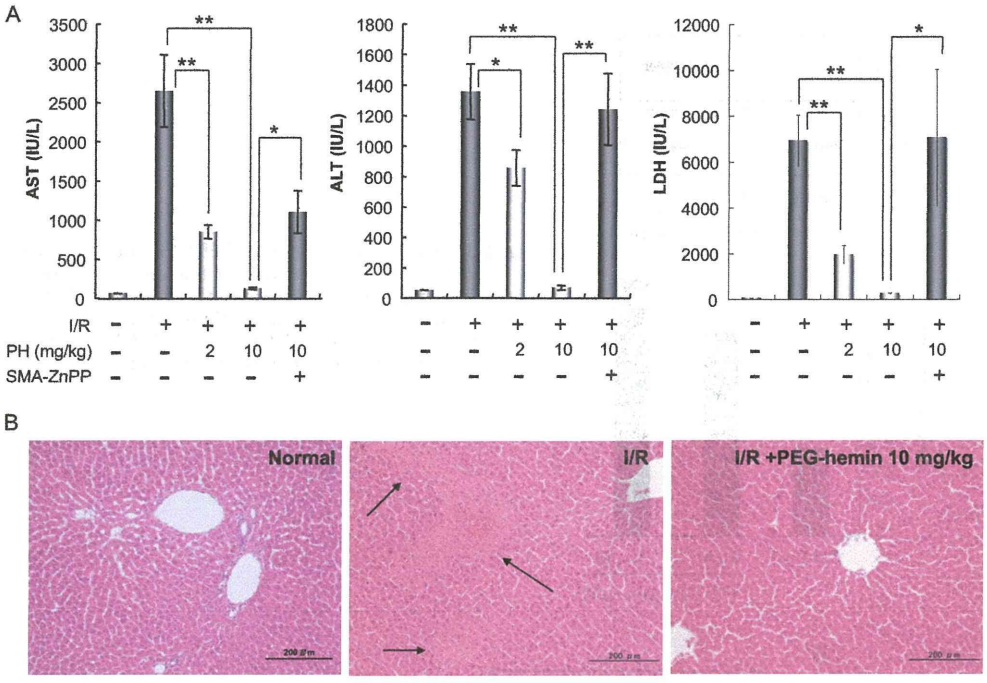

Fig. 6. Effect of PEG-hemin on hepatic I/R injury evaluated by changes in serum levels of AST, ALT, and LDH (A) and histological examination of rat liver tissue (B). Ischemia was induced by occluding both the portal vein and hepatic artery for 30 min followed by reperfusion for 3 h. PEG-hemin (PH) was administered intravenously 2 h before ischemia. The concentration of SMA-ZnPP administered to rats was 5 mg/kg. See *Amelioration of Liver I/R Injury by PEG-Hemin* under *Results* for details. Data are presented as means ± S.E. (n = 3–12). *, $P < 0.05$; **, $P < 0.01$. Arrows in B indicate necrotic areas of liver tissue.

AQ: T

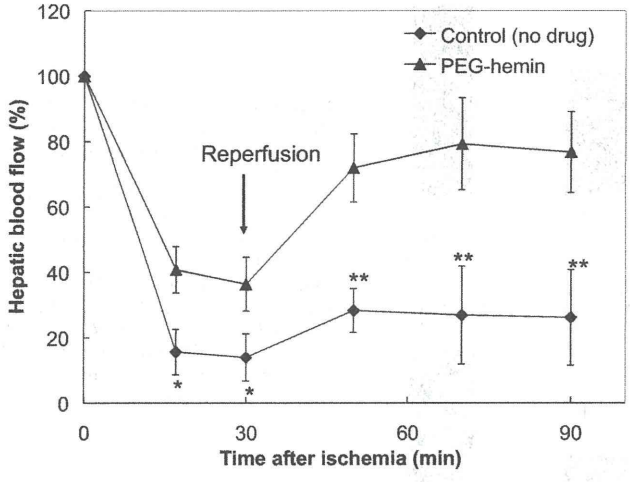

Fig. 7. Time profile of changes in hepatic blood flow before and after I/R and PEG-hemin treatment. Blood flow values are expressed as a percentage of the value measured before ischemia. PEG-hemin (10 mg/kg) was injected intravenously as noted in Fig. 6. Data are presented as means ± S.E. (n = 3–4). *, $P < 0.05$; **, $P < 0.01$, PEG-hemin versus native hemin.

(larger than 40 kDa) are known to have various beneficial characteristics including prolonged in vivo $t_{1/2}$ as shown above, and, what is more important, selective accumulation and retention in solid tumor and inflammatory tissues. This unique phenomenon of macromolecules was named the enhanced permeability and retention (EPR) effect (Matsumura and Maeda, 1986; Maeda et al., 2000, 2001; Duncan, 2003; Fang et al., 2011). Many macromolecular drugs have been developed on the basis of the EPR effect and are now not only at the laboratory stage of development but also in the clinical stage (Maeda et al., 2001; Duncan, 2003; Nagamitsu et al., 2009; Maeda, 2010; Fang et al., 2011).

In addition, the macromolecular PEG-hemin micelles showed relatively strong HO-1 induction activity, both in vitro and in vivo, as evidenced by mRNA and protein levels (Figs. 4B and 5A). More important was HO-1 enzymatic activity of generation of both antioxidative bilirubin and CO (Fig. 5, B and C), which are the essential components to exhibit the pharmacological effect of HO-1. By quantifying bilirubin production, one can assess the enzyme activity of HO. However, it may not reflect the physiological role of HO in vivo. Measurement of CO that is derived mostly from HO in biological organisms (Abraham and Kappas, 2008), in circulation, or tissues may thus useful to evaluate the physiological role of HO in vivo. The results presented in this study clearly indicated the correlation of the circulation CO level in parallel with HO expression and bilirubin production (Fig. 5). Further investigations are warranted for the measurement of CO levels in tissues.

Mechanisms involved in the tissue-protective and therapeutic effects of PEG-hemin were thought to rely mostly on the antioxidative role of HO-1, which would take advantage of the enzyme reactions in heme catabolism (Fang et al., 2004; Abraham and Kappas, 2008). Heme and free iron are pro-oxidants that would induce or enhance ROS generation (Akaike et al., 1992; Jeney et al., 2002), whereas bilirubin, which is a major product of heme degradation, is one of the most abundant endogenous antioxidants in mammals and accounts for the major antioxidative activity in human serum (Baranano et al., 2002).

More recently, CO generated during heme degradation is also believed to account for the major, if not all, biological properties of HO-1. HO-catalyzed heme catabolism is the major source of CO (i.e., more than 80%) in the mammalian system, and the roles of CO include, similarly to NO, regulating vascular tone (vasorelaxant), participating in antiapoptosis, serving an antioxidative, anti-inflammatory function, and inhibiting the activation of monocyte/macrophages, inducing angiogenesis, and others (Abraham and Kappas, 2008). In our present experiment, we found the CO concentration in circulation increased after PEG-hemin treatment (Fig. 5C), which was paralleled with the improved hepatic

COLOR

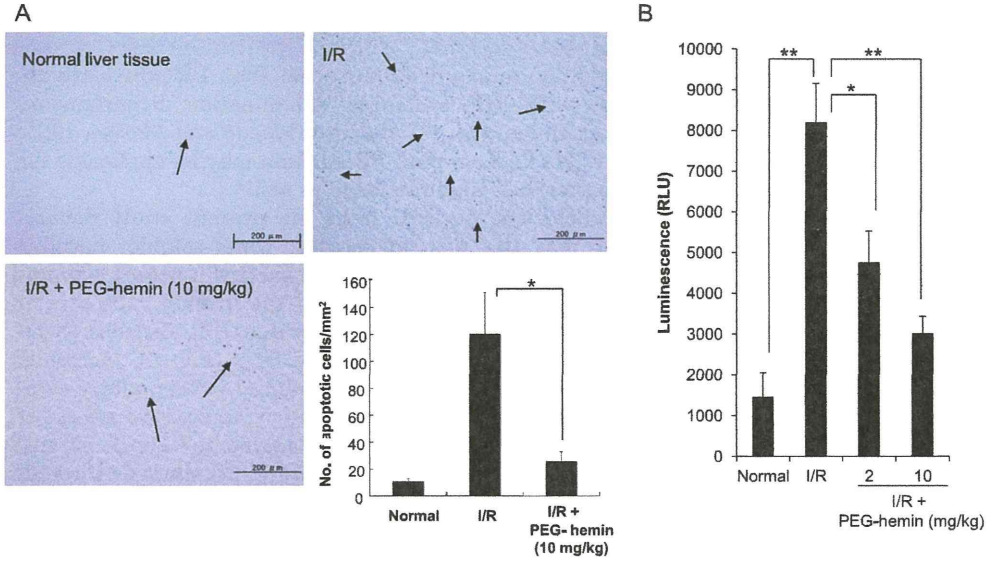

Fig. 8. Effect of PEG-hemin on I/R-induced apoptotic changes in the liver. Rats were treated with PEG-hemin before I/R, as given in Fig. 6. A, at 3 h after reperfusion, liver tissues were collected and paraffin-embedded sections were prepared for TUNEL staining (A). Arrows point to apoptotic cells. B, the caspase 3/7 activities in the liver tissues were also quantified. Data are presented as means ± S.E. (n = 3–6). *, $P < 0.05$; **, $P < 0.01$.

AQ: U

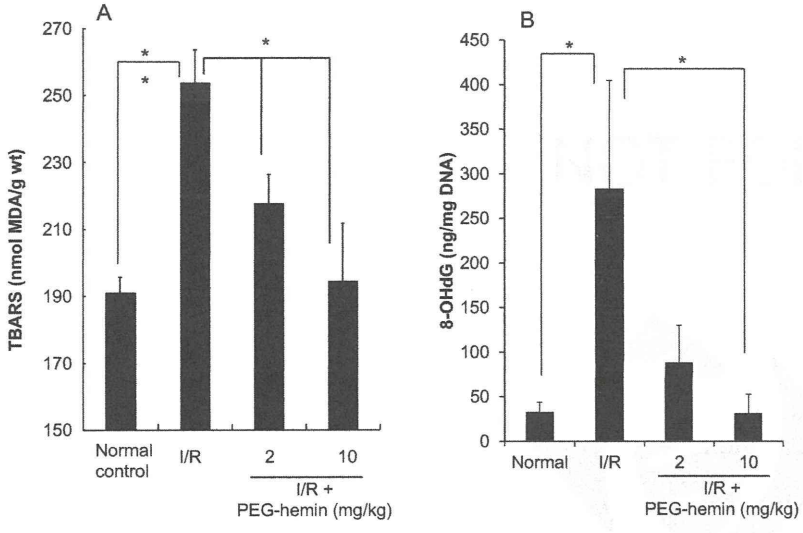

Fig. 9. TBARS (A) and 8-OHdG (B) in the rat liver after I/R injury with or without PEG-hemin treatment. The experimental protocol is the same as that noted in Fig. 6. At 3 h after reperfusion, rats were killed and the liver tissues were collected and subjected to the TBARS assay and ELISA of 8-OHdG (see *Materials and Methods* for details). Data are presented as means ± S.E. (n = 3–4). *, $P < 0.05$.

blood flow (Fig. 7) and decreased apoptosis in the liver in the I/R process (Fig. 8), even though we did not show direct evidence of its role on the cytoprotective effect against I/R injury. However, a recent study by Wei et al. (2010) demonstrated a direct effect of CO on I/R injury by using a CO-releasing molecule, although the effect was less significant, probably because of the short in vivo $t_{1/2}$ of CO-releasing agent.

In addition to HO-1 (the inducible enzyme), the constitutive form of HO, namely HO-2 is a major source of HO activity in most tissues. Both are alike in terms of enzymatic mechanisms of heme degradation and cofactor and substrate specificity (Maines, 1988; Abraham and Kappas, 2008). The HO activities in liver tissues measured in this study (Fig. 5B) may thus include HO-2 activity as well. Unlike HO-1, whose expression is relatively low in most normal tissues unless exposed to various stresses, such as I/R injury and hemin treatment as shown in this study (Fig. 5), HO-2 displays, in general, a constitutive expression in many normal tissues but it is not up-regulated upon stress or injury, which was also confirmed in this study (Supplemental Fig. 1). HO-2 is thus believed to contribute to normal housekeeping. And it has been reported that HO-2 behaves as a basal tone of anti-inflammatory signals, and deletion of HO-2 disables execution of the acute inflammatory and reparative response, leading to an exaggerated inflammatory response including increased oxidative stress and angiogenesis (Seta et al., 2006; Bellner et al., 2009). Moreover, it is known that HO-2 is induced by the treatment of corticosteroids (Maines et al., 1996), which is an important protective response during acute illness or stress, and is widely used as a treatment of inflammatory diseases. Thus, HO-2, along with HO-1, may also play important role as a protective response against I/R and inflammatory distress, facilitating the therapeutic response induced by PEG-hemin, which warranted further investigations.

I/R injury is a typical ROS-related inflammatory disorder, in which $O_2^{\cdot-}$, as a highly reactive radical, reacts with and oxidizes many biological molecules including NO (McCord, 1985; Maeda and Akaike, 1991; Ikebe et al., 2000) and thereby can trigger cell death. These pathological roles were clearly demonstrated in the present study using the I/R procedure, as evidenced by increased levels of the inflammatory cytokine MCP-1 (Fig. 10), elevated TBARS and 8-OHdG (Fig.

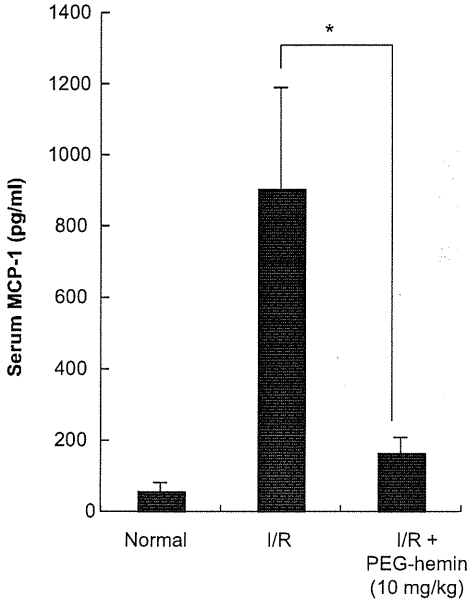

Fig. 10. Induction of MCP-1 by I/R injury and the protective effect of PEG-hemin. I/R and treatment protocols were the same as mentioned in Fig. 6. The serum MCP-1 concentration was measured by using an ELISA kit. Data are presented as means ± S.E. (n = 4–6). *, $P < 0.05$.

9), and apoptosis in liver tissue (Fig. 8), all of which were at least partly ameliorated by PEG-hemin treatment. As described above, O_2^- reacts extremely rapidly with NO at diffusion rate-dependent manner, and NO is thus removed and bioavailability of NO is reduced in the body, resulting in vascular constriction. These events explain, at least partly if not completely, the low hepatic blood flow after reperfusion during I/R, as Fig. 7 shows. Scavenging O_2^- will result in the reduction of apoptosis of hepatic cells and improve hepatic blood flow (Figs. 7 and 8). As a consequence, pathological effects caused by I/R injury will be prevented.

With regard to the treatment protocol in the present study, PEG-hemin was administered 2 h before ischemia was initiated, so as to achieve sufficient HO-1 induction, as shown in Fig. 5. This study used an acute I/R injury model, in which the injury peaked within 3 h, so that induction of HO-1 before I/R was necessary. Late treatment may be less effective because pathological changes progress quickly and may not be reversed before sufficient HO-1 expression. Acute I/R injury can in fact be observed in many medical interventions, such as routine operations, and especially organ transplantation, in which temporary obstruction of the blood flow of an organ or tissue is necessary, and the I/R injury of the tissue or organ is unavoidable and predictable. In these cases, prior administration of PEG-hemin and induction of HO-1 would be reasonable and practical and may produce successful therapeutic results. However, many I/R injuries seen in clinical settings are subacute or chronic, in which ROS are generated and injury progresses slowly but gradually; these situations include cardiac arrest, cerebral ischemia, thrombosis, and stroke (McCord, 1985). PEG-hemin may thus be beneficial in these cases with its long plasma half-life (Fig. 3; Table 1) and thus potent and sustained HO-1 induction activity. For groups at high risk of developing these diseases, PEG-hemin may become more important as a preventive medication because PEG-hemin itself demonstrated no or very little toxicity (Fig. 4A).

In addition, many disorders other than I/R injury are associated with ROS including inflammation, hypertension, and bacterial and viral infections (Maeda and Akaike, 1991; McCord, 2000). Therefore PEG-hemin may be applicable for the treatment of these diseases as well.

In conclusion, findings from the present study demonstrated that the macromolecular, water-soluble, micellar form of HO-1 inducer PEG-hemin exerted a potent cytoprotective effect against I/R injury of the liver in rats, as evidenced by low serum liver enzyme values (Fig. 6A), decreased numbers of apoptotic cells in the liver (Fig. 8), increased hepatic blood flow (Fig. 7), and reduced inflammatory cytokine levels in serum (Fig. 10). The cytoprotective effects of PEG-hemin can be attributed to augmented HO-1 activity (e.g., increased CO production, as Fig. 5C showed) through its antiapoptotic, antioxidative actions, because the HO-1 inhibitor SMA-ZnPP almost completely nullified the effect of PEG-hemin (Fig. 6A). This finding was also supported by the increased HO-1 mRNA and protein expression and elevated CO levels in blood and HO-1 enzyme activity (Figs. 4B and 5) and reduced tissue peroxidation in the liver after PEG-hemin treatment (Fig. 9). Therefore, the data presented herein suggest a therapeutic potential of PEG-hemin for I/R injury, and other ROS-related diseases, such as inflammatory disorders and hypertension, so PEG-hemin warrants further investigation as a therapeutic agent.

Acknowledgments

We thank Judith Gandy for editing the manuscript and Gahininath Y. Bharate for his excellent technical assistance.

Authorship Contributions AQ: M

Participated in research design: Fang and Maeda.

Conducted experiments: Fang, Qin, Seki, Nakamura, and Tsukigawa.

Wrote or contributed to the writing of the manuscript: Fang, Qin, and Maeda.

References

Abraham NG and Kappas A (2008) Pharmacological and clinical aspects of heme oxygenase. *Pharmacol Rev* **60:**79–127.

Akaike T and Maeda H (2000) Pathophysiological effects of high-output production of nitric oxide, in *Nitric Oxide: Biology and Pathology* (Ignarro LJ ed) pp 733–745, Academic Press, San Diego.

Akaike T, Sato K, Ijiri S, Miyamoto Y, Kohno M, Ando M, and Maeda H (1992) Bactericidal activity of alkyl peroxyl radicals generated by heme-iron-catalyzed decomposition of organic peroxides. *Arch Biochem Biophys* **294:**55–63.

Baranano DE, Rao M, Ferris CD, and Snyder SH (2002) Biliverdin reductase: a major physiologic cytoprotectant. *Proc Natl Acad Sci U S A* **99:**16093–16098.

Beckman JS and Koppenol WH (1996) Nitric oxide, superoxide, and peroxynitrite: the good, the bad, and ugly. *Am J Physiol Cell Physiol* **271:**C1424–C1437.

Beckman KB and Ames BN (1997) Oxidative decay of DNA. *J Biol Chem* **272:**19633–19636.

Bellner L, Martinelli L, Halilovic A, Patil K, Puri N, Dunn MW, Regan RF, and Schwartzman ML (2009) Heme oxygenase-2 deletion causes endothelial cell activation marked by oxidative stress, inflammation, and angiogenesis. *J Pharmacol Exp Ther* **331:**925–932.

Berlett BS and Stadtman ER (1997) Protein oxidation in aging, disease, and oxidative stress. *J Biol Chem* **272:**20313–20316.

Davies KJ (1995) Oxidative stress: the paradox of aerobic life. *Biochem Soc Symp* **61:**1–31.

Doi K, Akaike T, Fujii S, Tanaka S, Ikebe N, Beppu T, Shibahara S, Ogawa M, and Maeda H (1999) Induction of haem oxygenase-1 nitric oxide and ischaemia in experimental solid tumours and implications for tumour growth. *Br J Cancer* **80:**1945–1954.

Duncan R (2003) The dawning era of polymer therapeutics. *Nat Rev Drug Discov* **2:**347–360.

Fang J, Akaike T, and Maeda H (2004) Antiapoptotic role of heme oxygenase (HO) and the potential of HO as a target in anticancer treatment. *Apoptosis* **9:**27–35.

Fang J, Iyer AK, Seki T, Nakamura H, Greish K, and Maeda H (2009a) SMA-

copolymer conjugate of AHPP: a polymeric inhibitor of xanthine oxidase with potential antihypertensive effect. *J Control Release* **135:**211–217.

Fang J, Nakamura H, and Maeda H (2011) The EPR effect: Unique features of tumor blood vessels for drug delivery, factors involved, and limitations and augmentation of the effect. *Adv Drug Deliv Rev* **63:**136–151.

Fang J, Sawa T, Akaike T, Akuta T, Sahoo SK, Khaled G, Hamada A, and Maeda H (2003) In vivo antitumor activity of pegylated zinc protoporphyrin: targeted inhibition of heme oxygenase in solid tumor. *Cancer Res* **63:**3567–3574.

Fang J, Seki T, and Maeda H (2009b) Therapeutic strategies by modulating oxygen stress in cancer and inflammation. *Adv Drug Deliv Rev* **61:**290–302.

Fang J, Seki T, Qin H, Bharate GY, Iyer AK, and Maeda H (2010) Tissue protective effect of xanthine oxidase inhibitor, polymer conjugate of (styrene-maleic acid copolymer) and (4-amino-6-hydroxypyrazolo[3,4-*d*]pyrimidine), on hepatic ischemia-reperfusion injury. *Exp Biol Med (Maywood)* **235:**487–496.

Halliwell B and Gutteridge JM (1984) Free radicals, lipid peroxidation, and cell damage. *Lancet* **2:**1095.

Ikebe N, Akaike T, Miyamoto Y, Hayashida K, Yoshitake J, Ogawa M, and Maeda H (2000) Protective effect of *S*-nitrosylated α_1-protease inhibitor on hepatic ischemia-reperfusion injury. *J Pharmacol Exp Ther* **295:**904–911.

Iyer AK, Greish K, Fang J, Murakami R, and Maeda H (2007) High-loading nanosized micelles of copoly(styrene-maleic acid)-zinc protoporphyrin for targeted delivery of a potent heme oxygenase inhibitor. *Biomaterials* **28:**1871–1881.

Jeney V, Balla J, Yachie A, Varga Z, Vercellotti GM, Eaton JW, and Balla G (2002) Pro-oxidant and cytotoxic effects of circulating heme. *Blood* **100:**879–887.

Maeda H (2010) Tumor-selective delivery of macromolecular drugs via the EPR effect: background and future prospects. *Bioconjug Chem* **21:**797–802.

Maeda H and Akaike T (1991) Oxygen free radicals as pathogenic molecules in viral diseases. *Proc Soc Exp Biol Med* **198:**721–727.

Maeda H, Sawa T, and Konno T (2001) Mechanism of tumor-targeted delivery of macromolecular drugs, including the EPR effect in solid tumor and clinical overview of the prototype polymeric drug SMANCS. *J Control Release* **74:**47–61.

Maeda H, Wu J, Sawa T, Matsumura Y, and Hori K (2000) Tumor vascular permeability and the EPR effect in macromolecular therapeutics: a review. *J Control Release* **65:**271–284.

Maines MD (1988) Heme oxygenase: function, multiplicity, regulatory mechanisms, and clinical applications. *FASEB J* **2:**2557–2568.

Maines MD, Eke BC, and Zhao X (1996) Corticosterone promotes increased heme oxygenase-2 protein and transcript expression in the newborn rat brain. *Brain Res* **722:**83–94.

Matsumura Y and Maeda H (1986) A new concept for macromolecular therapeutics in cancer chemotherapy: mechanism of tumoritropic accumulation of proteins and the antitumor agent smancs. *Cancer Res* **46:**6387–6392.

McCord JM (1985) Oxygen-derived free radicals in postischemic tissue injury. *N Engl J Med* **312:**159–163.

McCord JM (2000) The evolution of free radicals and oxidative stress. *Am J Med* **108:**652–659.

Melgarejo E, Medina MA, Sánchez-Jiménez F, and Urdiales JL (2009) Monocyte chemoattractant protein-1: a key mediator in inflammatory processes. *Int J Biochem Cell Biol* **41:**998–1001.

Miyamoto Y, Akaike T, Yoshida M, Goto S, Horie H, and Maeda H (1996) Potentiation of nitric oxide-mediated vasorelaxation by xanthine oxidase inhibitors. *Proc Soc Exp Biol Med* **211:**366–373.

Muzykantov VR, Atochina EN, Ischiropoulos H, Danilov SM, and Fisher AB (1996) Immunotargeting of antioxidant enzyme to the pulmonary endothelium. *Proc Natl Acad Sci U S A* **93:**5213–5218.

Nagamitsu A, Greish K, and Maeda H (2009) Elevating blood pressure as a strategy to increase tumor-targeted delivery of macromolecular drug SMANCS: cases of advanced solid tumors. *Jpn J Clin Oncol* **39:**756–766.

Oda T, Akaike T, Hamamoto T, Suzuki F, Hirano T, and Maeda H (1989) Oxygen radicals in influenza-induced pathogenesis and treatment with pyran polymer-conjugated SOD. *Science* **244:**974–976.

Ohkawa H, Ohishi N, and Yagi K (1979) Assay for lipid peroxides in animal tissues by thiobarbituric acid reaction. *Anal Biochem* **95:**351–358.

Roy RS and McCord JM (1983) Superoxide and ischemia: conversion of xanthine dehydrogenase to xanthine oxidase, in *Oxyradicals and Their Scavenger Systems* (Greenwald R, and Cohen G eds) pp 145–153, Elsevier Science, New York.

Sahoo SK, Sawa T, Fang J, Tanaka S, Miyamoto Y, Akaike T, and Maeda H (2002) Pegylated zinc protoporphyrin: a water-soluble heme oxygenase inhibitor with tumor-targeting capacity. *Bioconjug Chem* **13:**1031–1038.

Sawa T, Wu J, Akaike T, and Maeda H (2000) Tumor-targeting chemotherapy by a xanthine oxidase-polymer conjugate that generates oxygen-free radicals in tumor tissue. *Cancer Res* **60:**666–671.

Seta F, Bellner L, Rezzani R, Regan RF, Dunn MW, Abraham NG, Gronert K, and Laniado-Schwartzman M (2006) Heme oxygenase-2 is a critical determinant for execution of an acute inflammatory and reparative response. *Am J Pathol* **169:**1612–1623.

Stocks SJ, Jones AJ, Ramey CW, and Brooks DE (1986) A fluorometric assay of the degree of modification of protein primary amines with polyethylene glycol. *Anal Biochem* **154:**232–234.

Wei Y, Chen P, de Bruyn M, Zhang W, Bremer E, and Helfrich W (2010) Carbon monoxide-releasing molecule-2 (CORM-2) attenuates acute hepatic ischemia reperfusion injury in rats. *BMC Gastroenterol* **10:**42.

Address correspondence to: Professor Hiroshi Maeda, DDS Research Institute, Sojo University, Kumamoto 860-0082, Japan. E-mail: hirmaeda@ph.sojo-u.ac.jp

AQ: N

IAI
Journals.ASM.org

Protective Role of D-Amino Acid Oxidase against *Staphylococcus aureus* Infection

Hideaki Nakamura,[a,b] Jun Fang,[a,b] and Hiroshi Maeda[b]

Laboratory of Microbiology and Oncology, Faculty of Pharmaceutical Science, Sojo University, Ikeda, Kumamoto, Japan,[a] and Institute for DDS, Sojo University, Ikeda, Kumamoto, Japan[b]

D-Amino acid oxidase (DAO) is a hydrogen peroxide-generating enzyme that uses a D-amino acid as a substrate. We hypothesized that DAO may protect against bacterial infection, because hydrogen peroxide is one of the most important molecules in the antibacterial defense systems in mammals. We show here that DAO suppressed the growth of *Staphylococcus aureus* in a manner that depended on the concentration of DAO and D-amino acid *in vitro*. Addition of catalase abolished the bacteriostatic activity of DAO. Although DAO plus D-Ala showed less bactericidal activity, addition of myeloperoxidase (MPO) greatly enhanced the bactericidal activity of DAO. Furthermore, DAO was able to utilize bacterial lysate, which contains D-Ala derived from peptidoglycan; this could produce hydrogen peroxide with, in the presence of myeloperoxidase, formation of hypochlorous acid. This concerted reaction of DAO and MPO led to the bactericidal action. *In vivo* experiments showed that $DAO^{-/-}$ (mutant) mice were more susceptible to *S. aureus* infection than were $DAO^{+/+}$ (wild-type) mice. These results suggest that DAO, together with myeloperoxidase, may play an important role in antibacterial systems in mammals.

Hydrogen peroxide (H_2O_2), a major reactive oxygen species (ROS), demonstrates bactericidal activity against various microorganisms (14). In mammals, immune cells (macrophages and neutrophils) utilize ROS, such as H_2O_2 and superoxide anion radical, to eliminate infecting bacteria. Furthermore, in the presence of H_2O_2, myeloperoxidase (MPO) oxidizes halide ions (Cl^- and I^-) to produce hypohalous acid (hypochlorous acid [HOCl] and hypoiodous acid). Hypohalous acid is one of the most active ROS and is toxic to various microbes. Neutrophils are major immune cells that utilize HOCl to eliminate infecting bacteria. For neutrophils, a primary source of the H_2O_2 used to generate HOCl is NADPH oxidase (24). H_2O_2 may also have an additional significant role in chronic granulomatous disease, which is a hereditary disease caused by abnormal H_2O_2 production in neutrophils that is primarily due to defective NADPH oxidase (7, 9).

D-Amino acid oxidase (DAO) is another H_2O_2-generating enzyme, which uses flavin adenine dinucleotide (FAD) as a coenzyme. Biochemically, DAO catalyzes oxidative deamination of D-amino acids to yield corresponding α-keto acids, with molecular oxygen (O_2) used as an electron acceptor and, thus, formation of H_2O_2. DAO exists in many organisms, from yeasts to mammals, but not in bacteria. In mammals, DAO is abundant in the kidney, liver, and brain. However, the biological roles of DAO in mammals remain unclear. In the brain, for example, DAO is associated with neurotransmission via modulation of D-serine levels. The enzymatic activity of DAO has been correlated with the incidence of schizophrenia (8).

Moreover, several researchers found DAO in human and porcine neutrophils, which suggests an important antibacterial role for DAO in neutrophils. Robinson et al. reported that DAO is located on the cell surface and DAO is internalized with foreign objects, such as bacteria (26). Reports that purified porcine DAO has antibacterial activity against *Escherichia coli in vitro* and that its activity was enhanced by addition of D-amino acids, as well as by binding of DAO to bacterial cell walls, have appeared in the literature (10, 29).

D-Amino acids (e.g., D-Ala and D-Glu) are integral components of the peptidoglycan of bacterial cell walls and are missing in mammals. We thus hypothesized that DAO may utilize D-Ala generated by target bacteria and that peptidoglycan synthesis may be involved in defense against microbial infections, because D-Ala is ubiquitous in bacteria. DAO activity is also reportedly absent in the kidney in most germ-free mice and is partially restored by injection of D-Ala (21), which suggests that DAO may be induced by cell wall components and thus may protect hosts against bacterial infection. However, some researchers reported no difference in DAO activity in germ-free mice and conventional mice (23).

In this study, we investigated the potential role of DAO as an antibacterial defense enzyme by using a porcine recombinant DAO, as well as *in vitro* and *in vivo* experiments with DAO-deficient mice and *Staphylococcus aureus*. The combined effect of DAO and MPO was also investigated.

MATERIALS AND METHODS

Materials. The *S. aureus* strain ATCC 25923 was used in this study. ddY mice were purchased from Japan SLC, Inc., Shizuoka, Japan. Soybean casein digest (SCD) broth was purchased from Nissui Co., Tokyo, Japan. Leupeptin, phenylmethylsulfonyl fluoride (PMSF), and FAD were purchased from Sigma-Aldrich Chemical Co., St. Louis, MO. 3-[(3-Cholamidopropyl)dimethylammonio]-1-propanesulfonate (CHAPS) and SBT [*N*,*N*′-bis (2,4-disulfobenzyl) toluidine] was purchased from Dojindo Chemical Laboratories, Kumamoto, Japan. TaKaRa Ex *Taq* was purchased from Takara Bio Inc., Shiga, Japan. PflMI restriction enzyme was purchased from New England BioLabs (Ipswich, MA). SCD agar, isopropyl-β-D-thiogalactopyranoside, carbenicillin, polyoxyethylene sorbitan

Received 1 December 2011 Returned for modification 2 December 2011
Accepted 12 January 2012
Published ahead of print 25 January 2012
Editor: S. R. Blanke
Address correspondence to Hiroshi Maeda, hirmaeda@ph.sojo-u.ac.jp.

doi:10.1128/IAI.06214-11

monolaurate (Tween 20), ammonium sulfate, Tris, EDTA, sodium dodecyl sulfate (SDS), proteinase K, casein sodium, and others were purchased from Wako Pure Chemical Industries, Ltd., Osaka, Japan.

Production and purification of recombinant DAO. Recombinant porcine DAO was prepared as described previously (12). Briefly, the *E. coli* BL21(DE3) strain harboring a pET3c plasmid encoding porcine DAO was cultured in LB medium containing 50 μg/ml carbenicillin as usual, and 0.01 mM isopropyl-β-D-thiogalactopyranoside was added to allow expression of DAO in *E. coli*. After culture for 20 h at 37°C, the bacterial pellets were sonicated (150 W; 30 min) in 20 mM pyrophosphate buffer (pH 8.2) at 4°C. DAO was obtained by means of ammonium sulfate precipitation after heat denaturation, followed by DEAE cellulose column chromatography. The purity of the DAO was checked by means of SDS-polyacrylamide gel electrophoresis (PAGE) with Coomassie brilliant blue staining (purity > 90%).

Assay for bacteriostatic and bactericidal activities. (i) Bacteriostatic activity. *S. aureus* was cultured until the mid-log phase of growth in SCD broth with reciprocal shaking at 1.5 Hz and 37°C. Then, the bacteria were washed twice with physiological saline (0.85%), and 1×10^6 CFU/ml of *S. aureus* was incubated with DAO (2 to 40 μg/ml), D-amino acids (D-Ala [1 to 10 mM], D-Pro [0.3 to 10 mM], D-Glu [10 mM], or D-Asp [10 mM]), and catalase (1 mg/ml) in SCD broth at 37°C for 5 h. The optical density at 570 nm was used to compare relative bacterial cell numbers for the different conditions tested.

(ii) Bactericidal activity. *S. aureus* (1×10^6 CFU/ml), which was prepared as described above, was incubated with DAO (10 to 200 μg/ml), D-amino acids in the same concentration range mentioned above, and MPO (3.2 U/ml) in 50 mM phosphate-citrate buffer (pH 5.5), or the bacteria were incubated with DAO (10 to 50 μg/ml) and the above-described D-amino acids in 10 mM phosphate-buffered saline (PBS) (pH 7.4) at 37°C in a shaking (1.5 Hz) water bath for 30 min. Duplicate 100-μl aliquots of each dilution were added to 15 ml of SCD agar and mixed well in petri dishes for colony formation. The numbers of colonies formed were determined after overnight incubation at 37°C.

Measurement of hydrogen peroxide production. Hydrogen peroxide was measured by colorimetric assay using peroxidase-coupled oxidation of *o*-dianisidine. DAO (5 μg/ml), bacterial lysate (0.5 to 1.0 mg/ml), and horseradish peroxidase (6.6 μg/ml) were incubated in 50 mM phosphate buffer (pH 7.4) containing *o*-dianisidine (75 μg/ml) at 25°C, and then absorbance at 460 nm was measured. Bacterial lysate was prepared by acid hydrolysis of *S. aureus*, hydrolysis in 6 M HCl at 110°C for 24 h, and was then kept in a desiccator containing pellets of NaOH under vacuum to remove the HCl and dried to obtain a powder.

Measurement of hypohalous acid generation. The amount of hypohalous acid (HOCl) was measured by a colorimetric method based on SBT. Briefly, an H_2O_2-generating system (200 μg/ml DAO and 10 mM D-Ala), 0.8 or 1.6 U/ml MPO, 200 mM NaCl, and 5 mg/ml potassium iodide were incubated with 0.1 mg/ml SBT in 50 mM phosphate citrate buffer (pH 5.5), after which the absorbance at 675 nm was measured (27). In another experiment, a lysate of *S. aureus* was used instead of D-Ala.

Genotyping. Genomic DNA was extracted from the auricles of ddY mice after incubation of auricular tissue in lysis buffer (10 mM Tris-HCl, 10 mM EDTA, 0.5% SDS, 0.5 mg/ml proteinase K) at 55°C for 6 h, after which the genomic DNA was purified by phenol-chloroform extraction and ethanol precipitation. The mouse *Dao* gene was amplified by means of PCR using 5′-mDAO and 3′-mDAO primers. The PCR products were also subjected to phenol-chloroform extraction and ethanol precipitation, followed by digestion with the restriction enzyme PflMI. The digested DNA fragments were then separated using 1% agarose gel electrophoresis. The primer sequences used for mouse *Dao* genotyping were as follows: 5′-mDAO, ATGTACGAAGCTGGAGGACAGAGGGG, and 3′-mDAO, CAAGCAGACAGGGCAAGCTCTTCATGG.

Quantification of bactericidal activity in kidneys. Six-week-old female ddY mice were injected with 1×10^7 CFU of *S. aureus* via the tail vein. Three days after bacterial challenge, the mice were sacrificed and the kidneys were excised. The kidneys were homogenized in 1% CHAPS in RPMI medium, and the homogenates were serially diluted with physiological saline. Duplicate 100-μl aliquots of each dilution were added to 15 ml of SCD agar at about 45°C and mixed vigorously in petri dishes. The numbers of viable bacteria were assessed by counting the colonies formed on SCD agar plates after overnight incubation at 37°C.

Measurement of DAO enzymatic activity. Kidneys or peritoneal neutrophils were homogenized using a Polytron homogenizer (Kinematica AG, Lucerne, Switzerland) or by ultrasonication (type Dr. Hielscher, UP50H homogenizer, tip drip type) in ice-cold suspension buffer (100 mM Tris-HCl, pH 8.0) containing a mixture of protease inhibitors (1 mM PMSF, 10 μg/ml leupeptin, and 2.5 mM EDTA). The tissue lysates obtained were then centrifuged (12,000 × *g*; 15 min at 4°C), and each supernatant specimen was used for measurement of DAO enzymatic activity. The DAO activity in the tissue lysates was determined on the basis of formation of α-keto acid (pyruvic acid) during the reaction between D-Ala and DAO, as described previously (11).

Preparation of mouse peritoneal neutrophils. Mouse peritoneal neutrophils were elicited by using a peritoneal injection of 3 ml of 6% casein sodium salt dissolved in physiological saline and harvested via peritoneal lavage 6 h later with 5 ml of PBS. Contaminating erythrocytes were removed by causing them to burst in hypotonic saline solution (0.2% NaCl); isotonicity was then restored with a rebalancing solution (1.9% NaCl), followed by centrifugation. Approximately 1×10^7 neutrophils were obtained from 10-week-old female ddY mice. The purity of the neutrophils was evaluated by means of Giemsa staining under a microscope.

Bactericidal activity of mouse neutrophils with wild-type ($DAO^{+/+}$) and DAO-deficient ($DAO^{-/-}$) mice. *S. aureus* bacteria at the mid-log phase in SCD broth as described above were washed twice with physiological saline and suspended in PBS containing 1 mM $MgCl_2$ and 1.5 mM $CaCl_2$, and the bacteria were treated with 10% pooled mouse serum at 37°C for 15 min for endocytosis after opsonization of *S. aureus* with mouse serum. Then, neutrophils were added to the bacteria at a 1:1 ratio of bacteria to neutrophils (4×10^6 cells/ml) in PBS supplemented with 1 mM glucose and 10% mouse serum for opsonization and incubated at 37°C. After 90 min of incubation, each sample was diluted in 0.2% Tween 20 and incubated for 5 min at room temperature to lyse the neutrophils and release phagocytosed bacteria, after which samples were vortexed vigorously and duplicate 100-μl aliquots were plated on 15-ml agar gel plates of SCD medium, followed by overnight culture at 37°C. The viable bacteria were then counted.

RESULTS

***In vitro* bacteriostatic activity of DAO.** We first examined the bacteriostatic activity of DAO against *S. aureus*. *S. aureus* bacteria were incubated with porcine DAO at various concentrations in the presence of 10 mM D-Ala in SCD medium. A concentration of 2 μg/ml DAO showed 50% bacterial growth suppression, and complete growth suppression was observed with DAO at more than 10 μg/ml (Fig. 1a). Similar concentration-dependent bacteriostatic activity was seen with D-Ala in the presence of 10 μg/ml of DAO (Fig. 1b). This bacteriostatic activity of DAO was not observed with the addition of L-Ala (Fig. 1a). Further, addition of 1 mg/ml catalase abolished the bacteriostatic effect of DAO completely (Fig. 1c), which suggests that H_2O_2 is the major effector of DAO-induced bacteriostatic effects. Though addition of D-Glu and D-Asp could not suppress *S. aureus* bacterial growth, D-Pro suppressed the growth of *S. aureus* more extensively than D-Ala in a dose-dependent manner (Fig. 1d and e).

Enhancement of the bactericidal effect of DAO with MPO *in vitro*. We also examined the bactericidal activity of DAO against *S. aureus*. DAO showed only weak bactericidal activity, even in the presence of 5 mM D-Ala; about 40% decreases in viable bacteria were observed (Fig. 2a). Next, we examined the bactericidal activ-

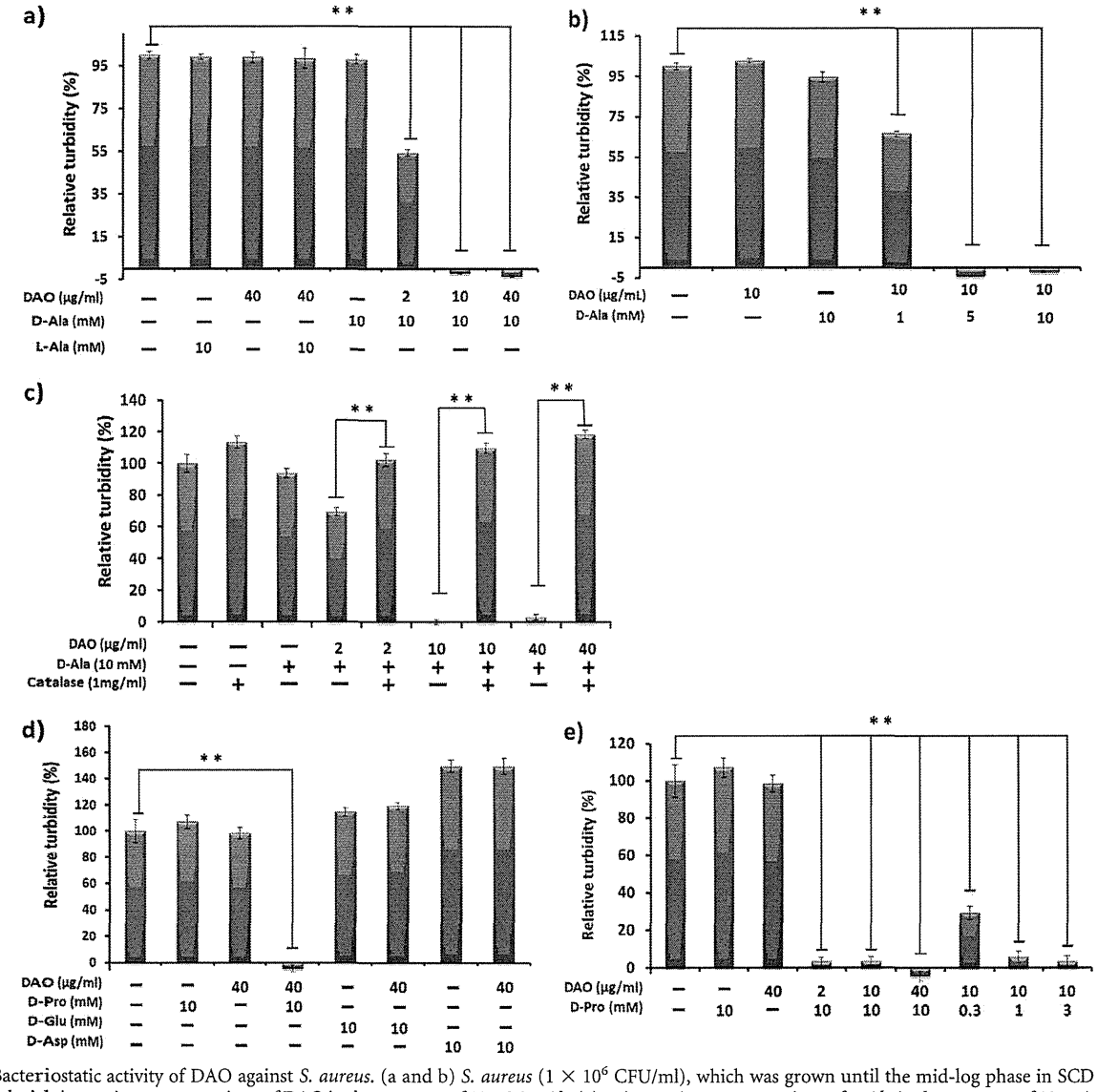

FIG 1 Bacteriostatic activity of DAO against *S. aureus*. (a and b) *S. aureus* (1×10^6 CFU/ml), which was grown until the mid-log phase in SCD broth, was incubated with increasing concentrations of DAO in the presence of 10 mM D-Ala (a) or increasing concentrations of D-Ala in the presence of 10 μg/ml DAO (b) in SCD broth at 37°C for 5 h, and then the optical density at 570 nm was measured. (c) *S. aureus* (1×10^6 CFU/ml) was incubated with DAO and D-Ala, with or without 1 mg/ml (5,000 to 10,000 U/ml) of bovine catalase, and then the optical density at 570 nm was measured. (d and e) *S. aureus* (1×10^6 CFU/ml) was incubated with DAO in the presence of D-amino acids (D-Pro [0.3 to 10 mM], D-Glu [10 mM], or D-Asp [10 mM]) in SCD broth at 37°C for 5 h, and then the optical density at 570 nm was measured. The values are means and standard deviations (SD). **, statistically significant differences ($P < 0.01$) by Student's *t* test.

ity of DAO in relation to that of MPO. Generation of hypohalous acid was detected by means of the SBT-based colorimetric method as described in Materials and Methods (27). Hypohalous acid was generated when the H_2O_2-generating system (DAO and D-Ala) was mixed with MPO and chloride ion (Fig. 2b). These results indicated that DAO serves as an H_2O_2 donor for MPO to generate HOCl.

We next examined the bactericidal activity of the DAO-MPO system. DAO alone showed no bactericidal activity at pH 5.5, but coincubation of DAO and D-Ala showed significant bactericidal activity; about 60% bacterial killing was achieved compared with the control under our experimental conditions (Fig. 2c, lane 7). When three components, DAO, D-Ala, and MPO, were incubated with bacteria, the highest bactericidal activity (more than 99% killing) among the conditions tested was obtained (Fig. 2c, lanes 10 to 14). Similar results were obtained using D-Pro; coincubation of D-Pro, DAO, and MPO showed the highest bactericidal activity against *S. aureus* (Fig. 2e and f); however, this was not the case with D-Glu and D-Asp (Fig. 2d and e).

Use of bacterial D-amino acid by DAO and generation of HOCl in the presence of MPO. Essentially all bacteria produce D-amino acids for the biosynthesis of peptidoglycan, the crucial component of the bacterial cell wall. We investigated whether DAO can use the bacterial lysate, which contains D-amino acids. Use of a D-amino acid, such as D-Ala, for DAO was examined by measuring the production of pyruvic acid, as well as generation of H_2O_2. Acid hydrolysate of *S. aureus* was used as the source of the bacterial D-amino acid. Incubation of the lysate with DAO led to

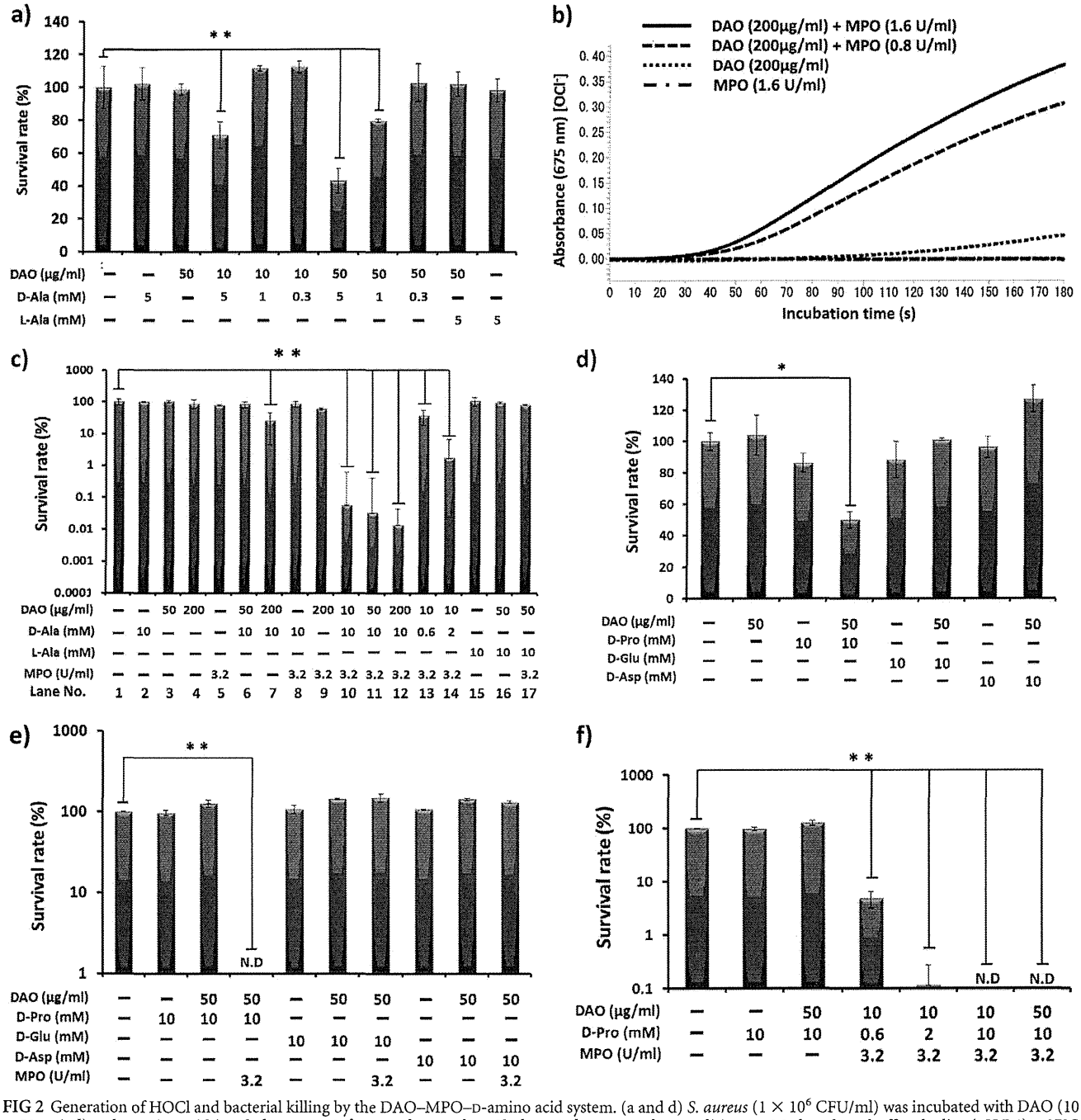

FIG 2 Generation of HOCl and bacterial killing by the DAO–MPO–D-amino acid system. (a and d) *S. aureus* (1×10^6 CFU/ml) was incubated with DAO (10 to 50 μg/ml) and D-amino acid (D-Ala [0.3 to 5 mM], D-Pro [10 mM], D-Glu [10 mM], or D-Asp [10 mM]) in 10 mM phosphate-buffered saline (pH 7.4) at 37°C for 30 min, and then each reaction mixture was diluted in physiological saline, mixed with warm SCD agar, and plated on petri dishes. The bacterial colonies were counted after overnight culture at 37°C. The values are expressed relative to the control. (b) DAO (200 μg/ml) was incubated with or without MPO in 50 mM phosphate citrate buffer (pH 5.5) for the indicated time in the system containing 10 mM D-Ala and 0.1 mg/ml SBT, an indicator of HOCl generation, and absorbance at 675 nm was then measured. (c, e, and f) *S. aureus* (1×10^6 CFU/ml) was incubated with a combination of DAO (10 to 200 μg/ml), D-amino acid (D-Ala [0.6 to 10 mM], D-Pro [0.6 to 10 mM], D-Glu [10 mM], or D-Asp [10 mM]), and MPO (3.2 U/ml) for 30 min in 50 mM phosphate citrate buffer (pH 5.5). The viable bacteria were counted by colony-forming assay as described above. The values are means and SD. N.D., not detected. ** and *, statistically significant differences ($P < 0.01$ and $P < 0.05$, respectively) by Student's *t* test.

significantly increased pyruvic acid production (Fig. 3a). Furthermore, generation of H_2O_2 was measured by incubation of the lysate of *S. aureus* and DAO (Fig. 3b), and HOCl was also generated in the presence of MPO (Fig. 3c). Indeed, coincubation with bacterial lysate, DAO, and MPO produced significant bactericidal activity (Fig. 3d). These results indicate that DAO can utilize bacterial lysates as a source of D-amino acid to generate H_2O_2, which is converted HOCl by MPO.

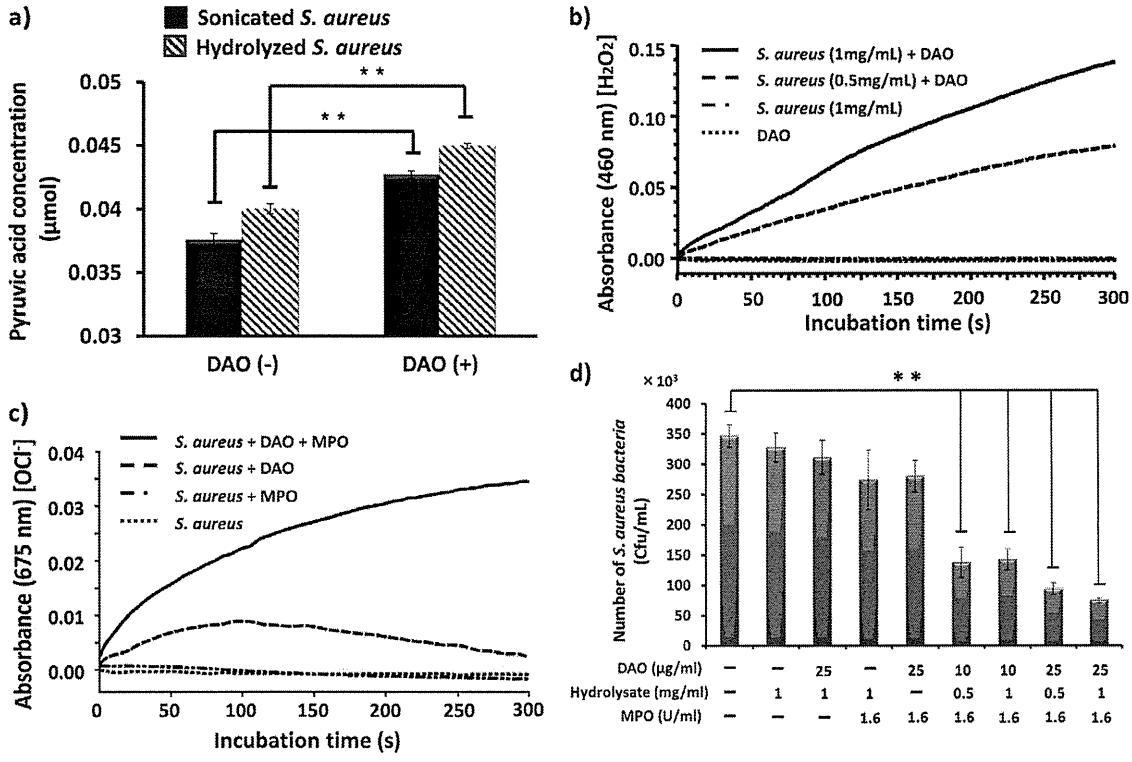

FIG 3 Utilization of bacterial cell wall-derived D-amino acid by DAO and generation of the bactericidal molecule HOCl. (a) Lysate of *S. aureus* (1 mg/ml) was incubated with 0.2 mg/ml DAO for 30 min at 37°C, and then pyruvic acid production was quantified as described in Materials and Methods. (b) Lysate of *S. aureus* (0.5 to 1 mg/ml) was incubated with DAO (5 μg/ml) in 50 mM phosphate buffer at 25°C for the indicated time to generate H_2O_2. H_2O_2 was measured by use of peroxidase-coupled oxidation of *o*-dianisidine (460 nm) as described in Materials and Methods. (c) Lysate of *S. aureus* (1 mg/ml) was incubated with DAO (200 μg/ml) plus MPO (1.6 U/ml) in the presence of SBT in acetate buffer (pH 5.5), and then absorbance at 675 nm was measured for HOCl generation. (d) *S. aureus* (1×10^6 CFU/ml) was incubated with the lysate of *S. aureus* (0.5 to 1.0 mg/ml), DAO (10 to 25 μg/ml), and MPO (1.6 U/ml) in 50 mM phosphate citrate buffer (pH 5.5) at 37°C for 30 min. Each reaction mixture was diluted with physiological saline, mixed with warm SCD agar, and plated on petri dishes. The bacterial colonies were counted after overnight culture at 37°C. The values are means and SD. **, statistically significant differences ($P < 0.01$) by Student's *t* test.

Difference in DAO activitin in $DAO^{+/+}$ and $DAO^{-/-}$ mice and their susceptibilities to bacterial infection. Certain ddY mice reportedly have a single-nucleotide substitution (541 G→A) in the *Dao* gene (Fig. 4a) (19). This nucleotide polymorphism results in the glycine (GGG)-to-arginine (AGG) amino acid substitution, which inactivates the enzyme activity of mouse DAO (19). We therefore sorted ddY mice into wild-type ($DAO^{+/+}$) and DAO-deficient ($DAO^{-/-}$) mice by using a restriction fragment length polymorphism (RFLP) method (Fig. 4b). Among 46 female ddY mice from Japan SLC, Inc., that were tested, 6 were wild-type mice (+/+), 16 were homozygous mutant mice (−/−), and 24 were heterozygous mice (+/−).

DAO activity in kidneys of ddY mice with different DAO expression levels was measured as described in Materials and Methods. Consistent with the results of *Dao* genotyping, DAO enzyme activity in the kidneys of $DAO^{+/+}$ mice was highest, and the lowest DAO activity occurred in kidneys of $DAO^{-/-}$ mice (56.9 mU/g wet tissue versus 0.04 mU/g wet tissue). $DAO^{+/-}$ mice showed about half the wild-type DAO activity (21.7 mU/g wet tissue) (Fig. 4c). To investigate the susceptibilities of mice with different DAO expression levels, ddY mice were injected intravenously (i.v.) with *S. aureus* via the tail vein as a renal bacterial infection model, and the number of viable bacteria in the kidneys was determined. The numbers of viable bacteria in the kidneys of the $DAO^{+/+}$ and $DAO^{+/-}$ mice were significantly reduced (to about 10%) compared with the numbers in the kidneys of $DAO^{-/-}$ mice (Fig. 4d). No significant difference was seen between $DAO^{+/+}$ and $DAO^{+/-}$ mice. We also examined the survival rate of ddY mice infected with *S. aureus*. After 2 weeks, 2 of 9 $DAO^{-/-}$ mice survived, whereas 5 of 9 $DAO^{+/+}$ mice survived (Fig. 4e).

DAO activity and bactericidal activity of neutrophils derived from DAO variant mice. We also examined the DAO activity of peritoneal neutrophils derived from $DAO^{+/+}$ and $DAO^{-/-}$ mice. The DAO activity of neutrophils derived from $DAO^{-/-}$ mice was 9.4 μU/mg protein, whereas that of neutrophils derived from $DAO^{+/+}$ mice was 125 μU/mg protein (Fig. 5a). Incubation with mouse peritoneal neutrophils dramatically reduced the viability of *S. aureus*, although no significant difference was seen between $DAO^{+/+}$ and $DAO^{-/-}$ mice (Fig. 5b).

DISCUSSION

In our previous studies, we reported that DAO showed selective cytotoxicity against various cancer cells *in vitro* and *in vivo* (12, 13). DAO-mediated cytotoxicity was nullified by the addition of catalase, which suggested that DAO exerted cytotoxic effects via production of H_2O_2. In this study, we examined the potential bacteriostatic and bactericidal activities of DAO *in vitro* and *in vivo*, as well as the role of DAO in MPO-dependent killing. For this

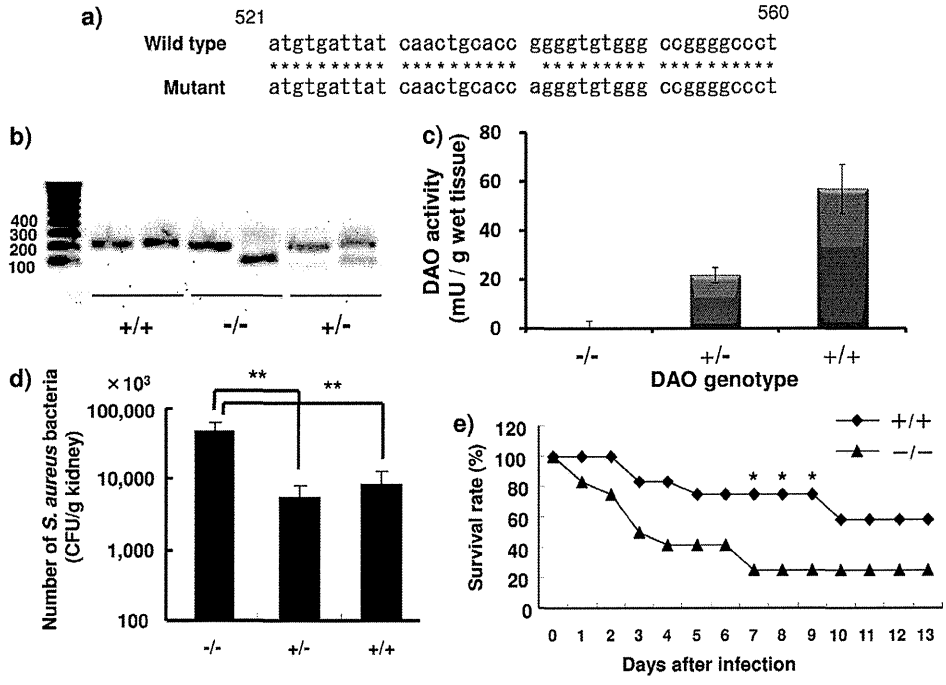

FIG 4 The *Dao* variant gene in ddY mice and its role in bacterial infection. (a) DNA sequences of the *Dao* genes in wild-type ($DAO^{+/+}$) and mutant ($DAO^{-/-}$) mice. Asterisks indicate identical nucleotide sequences. (b) The mouse *Dao* gene was amplified via a pair of 5′-mDAO and 3′-mDAO primers, followed by digestion with PflMI restriction enzyme. These digested fragments were applied to gel electrophoresis in a 1% agarose gel. (c) DAO activity in kidney homogenates was measured as described in Materials and Methods. (d) Fate of *S. aureus* after injection of 1×10^7 CFU/mouse. Three days after i.v. bacterial infection, viable bacteria in kidney homogenates were counted as described in Materials and Methods ($n = 7$ to 8). The values are means and SD. **, statistically significant differences ($P < 0.01$) by Student's *t* test. (e) Female ddY mice, 6 weeks old, were injected with *S. aureus*, 1×10^8 CFU/mouse, via the tail vein. The survival rates of the $DAO^{+/+}$ and $DAO^{-/-}$ groups were checked daily ($n = 9$). *, statistically significant differences ($P < 0.05$) by the chi-square test.

purpose, we prepared recombinant DAO obtained from different sources (i.e., pig, mouse, and human). We found that porcine DAO yielded both more DAO and higher enzyme activity than did the other DAOs (data not shown). We therefore utilized recombinant porcine DAO for our *in vitro* study. The recombinant DAO showed a single band, as judged from an SDS-PAGE gel stained with Coomassie brilliant blue. The relative activity of recombinant DAO was 5.3 U/mg protein, which is equivalent to that of purified DAO from porcine kidney.

In the present study, we observed that in the presence of 10 mM D-Ala, DAO showed concentration-dependent bacteriostatic activity against *S. aureus*, with the 50% inhibitory concentration (IC_{50}) of DAO almost 2 μg/ml (Fig. 1a). In the presence of 2 μg/ml of DAO, D-Ala showed a concentration-dependent bacteriostatic effect, and incubation of *S. aureus* with more than 5 mM D-Ala completely suppressed bacterial growth (Fig. 1b). Such DAO-mediated bacteriostatic activity was abolished by addition of catalase (Fig. 1c). This result clearly indicates the important role of H_2O_2 in the bacteriostatic activity of DAO. In this setting, L-Ala, D-Glu, and D-Asp did not show any bacteriostatic activity toward *S. aureus* even in the presence of DAO (Fig. 1a and d). This is because L-Ala, D-Glu, and D-Asp are not preferred substrates for DAO, and thus, there was no production of H_2O_2. D-Pro, which is a preferable substrate for DAO, showed more potent bacteriostatic activ-

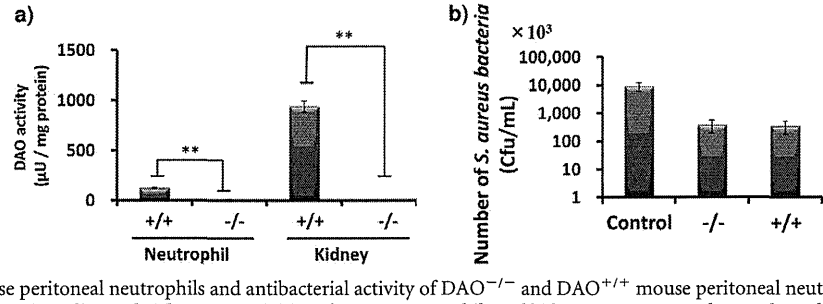

FIG 5 DAO activity of mouse peritoneal neutrophils and antibacterial activity of $DAO^{-/-}$ and $DAO^{+/+}$ mouse peritoneal neutrophils. (a) Peritoneal neutrophils were elicited using 6% casein sodium salt. The DAO activities of mouse neutrophils and kidney were measured, as evaluated by pyruvic acid formation. (b) *S. aureus* (4×10^6 CFU/ml) was incubated with or without equal numbers of mouse peritoneal neutrophils (1:1) at 37°C for 30 min. Serial dilutions were mixed with SCD agar on petri dishes, and the bacterial colonies were counted after overnight culture at 37°C. The values are means and SD. **, statistically significant differences ($P < 0.01$) by Student's *t* test.

ity against *S. aureus* (Fig. 1d and e). These results indicate that DAO needs available D-amino acids, such as D-Ala or D-Pro, to exhibit bacteriostatic activity.

Compared to the bacteriostatic activity of DAO, the bactericidal activity of D-Ala plus DAO was very weak (Fig. 2a and d);10 μg/ml DAO plus 5 mM D-Ala decreased the viable bacteria only to about 35%, at which point growth of *S. aureus* was completely suppressed (Fig. 1a and b). We further examined the bactericidal activity of the combination of DAO and MPO. MPO is an abundant protein in neutrophils (~5% of cellular protein) and is rich in granules (4). MPO is also found in the extracellular compartment after degranulation of granules (15). The biochemical function of MPO is oxidation of the Cl^- using H_2O_2 under acidic pH to produce HOCl. The resultant HOCl shows highly potent bactericidal activity (1).

In the present study, we showed that incubation of DAO and D-Ala with MPO in the presence of chloride ion at pH 5.5 generated HOCl (Fig. 2a). In this assay system, H_2O_2 was supplied via the reaction of DAO with D-Ala, after which MPO oxidized the chloride ion to generate HOCl. We then showed the bactericidal activity of DAO in combination with MPO. It was realized that MPO significantly enhanced the bactericidal activity of DAO when D-Ala or D-Pro was present (Fig. 2). Maximum bactericidal activity was observed when *S. aureus* was incubated with DAO, D-pro followed by D-Ala, and MPO; more than 99% of *S. aureus* bacteria were killed (Fig. 2c). Concerted bactericidal activity of DAO and MPO was not observed with the addition of L-Ala, D-Glu, or D-Asp (Fig. 2c and e) because these three amino acids are not preferable substrates for DAO reaction.

Peptidoglycan of *S. aureus* consists of alternating units of *N*-acetylglucosamine and *N*-acetylmuramic acid and a pentapeptide containing L-Ala, D-Ala, and D-Glu for structural integrity (28). D-Ala and D-Glu are generated by amino acid racemase and also by D-amino acid transaminase in bacteria (25). We next examined the availability of D-amino acids derived from bacteria for the substrate of DAO. By the incubation of bacterial lysate with DAO, the levels of pyruvic acid, a reaction product of DAO plus D-Ala, and H_2O_2 were elevated (Fig. 3a and b). Generation of H_2O_2 was observed by incubation of DAO and bacterial lysate, although the level of H_2O_2 was not sufficient to suppress the growth of *S. aureus* in SCD broth (data not shown). However, in the presence of MPO, concerted bactericidal activity against *S. aureus* was observed with DAO plus MPO and bacterial lysate. Namely, mixing of DAO (25 μg/ml), MPO (1.6 U/ml), and bacterial lysate (1 mg/ml) showed 80% killing of viable bacteria, whereas without MPO no bactericidal activity was observed (Fig. 3d). Thus, this bactericidal activity is thought to be mediated by the generation of HOCl (Fig. 3c). In fact, according to the literature, the culture medium of *S. aureus* contains D-amino acids at the mM level. The availability of D-Ala for DAO to utilize for the generation of H_2O_2 is considered to come from *de novo*-synthesized (by racemase) D-Ala. Importantly, DAO and MPO reportedly bind to bacterial cell walls and exhibit bacteriostatic and bactericidal activities (2, 29). This cell wall-binding property is advantageous for more localized and concentrated generation of antibacterial molecules, such as H_2O_2 and HOCl (2, 29). These results thus indicate that DAO and MPO can act synergistically in an antibacterial system.

Konno and Yasumura reported genetic polymorphism in the *Dao* gene in ddY mice (19). A fraction of ddY mice possess a single-nucleotide polymorphism in the *Dao* gene: a nucleotide change from GGG to AGG, which causes a glycine-to-arginine amino acid substitution. This amino acid substitution disrupted DAO enzyme activity without affecting the DAO expression level (19). We thus grouped ddY mice on the basis of genetic polymorphism by using the RFLP method, as described previously. Of 46 female ddY mice, 16 were double mutants ($DAO^{-/-}$), 24 were heterozygous ($DAO^{+/-}$), and 6 were wild type ($DAO^{+/+}$). In agreement with genotyping of the *Dao* gene, $DAO^{-/-}$ mice showed the lowest DAO activity (0.04 mU/g wet tissue) and $DAO^{+/+}$ mice had the highest DAO activity (56.9 mU/g wet tissue). $DAO^{+/-}$ mice had almost half the DAO activity (21.7 mU/g wet tissue) of $DAO^{+/+}$ mice.

We also examined the antibacterial role of DAO in an *in vivo* setting using $DAO^{+/+}$ and $DAO^{-/-}$ mice. Intravenous injection of *S. aureus* resulted in severe renal infection. Compared with $DAO^{-/-}$ mice, $DAO^{+/+}$ mice had significantly reduced (to less than 10%) numbers of viable bacteria in the kidney (Fig. 4d). Consistent with this result, $DAO^{+/+}$ mice demonstrated greater resistance to *S. aureus* infection (i.e., had a higher survival rate) than $DAO^{-/-}$ mice (Fig. 4e).

The neutrophil is one of the most important defenses against microbial infection, and its dysfunction causes severe chronic infection (3, 17). Therefore, we examined whether neutrophils derived from $DAO^{-/-}$ mice had lower bactericidal activity than neutrophils derived from $DAO^{+/+}$ mice. In fact, peritoneal neutrophils derived from $DAO^{+/+}$ mice showed higher DAO activity than did those derived from $DAO^{-/-}$ mice (Fig. 5a). However, contrary to our expectation, no difference in bactericidal activity was observed for neutrophils derived from $DAO^{+/+}$ and those derived from $DAO^{-/-}$ mice (Fig. 5b). This result may be due to the relatively low H_2O_2 generation potential of DAO compared with NADPH oxidase, which is the major source of H_2O_2 in neutrophils. DAO may not affect the net amount of H_2O_2 in neutrophils, and thus, it may not be the primary antibacterial component in neutrophils. However, it may be one component operating in antimicrobial defense, which may become important in specific cases, for example, NADPH oxidase deficiency. As mentioned above, DAO activity was higher in the kidneys of $DAO^{+/+}$ and $DAO^{+/-}$ mice, about 56.9 mU/g wet tissue and 21.7 mU/g wet tissue, respectively, than in $DAO^{-/-}$ mice. This activity is thought to be enough to reduce bacterial growth in the kidney, because a DAO concentration of 10 μg/ml suppressed bacterial growth, as shown in Fig. 1a and b. However, we could not show direct evidence that kidney homogenates exhibit bactericidal activity toward *S. aureus* (data not shown). This may be because, in this experimental workup, cellular integrity was completely destroyed, and formation of a phagosome and accumulation of antibacterial protein and supply of D-Ala at a localized site were not complete enough to show bactericidal activity, although more studies are needed to confirm this possibility. In this regard, Zhang et al. reported the potential binding of DAO to bacterial cell walls, and DAO showed higher antibacterial activity than a theoretical amount of H_2O_2, as calculated from the unit activity of DAO (30). Such H_2O_2 generation in the vicinity of bacteria may be advantageous for avoiding H_2O_2 degradation by kidney catalase before the H_2O_2 can act against the bacteria. Furthermore, neutrophils are recruited to the infected site, and abundant MPO may be available at sites of bacterial infection, which can exert the synergistic effect of DAO with MPO. In fact, in this study, we found that $DAO^{+/+}$

mice had less infection in the kidney and a higher survival rate after intravenous infection with *S. aureus* than $DAO^{-/-}$ mice.

S. aureus, used in the present study, is a catalase-producing bacterium and so is able to degrade H_2O_2 to water and oxygen. Production of catalase is well correlated with susceptibility to hydrogen peroxide treatment and with virulence and survival in the polymorph nuclear phagocyte (16, 22), though catalase-negative *S. aureus* may be more susceptible to treatment with DAO, D-Ala, and MPO, which remains to be elucidated. We also noticed that catalase-negative bacteria, such as *Streptococcus* spp., were more resistant to hydrogen peroxide treatment and DAO treatment (data not shown). This may be due to other anti-ROS enzymes, such as peroxidases, filling the role of catalase (6).

Based on the results shown in Fig. 1 and 2, DAO requires free D-amino acids, such as D-Ala or D-Pro, in order to exert bacteriostatic and bactericidal activities. Two D-amino acid sources of supply may be available in the *in vivo* setting: the infecting and growing bacteria and the enterobacteria. It has been reported that *S. aureus* possesses DAO-reactive materials, free D-amino acid, in the cell pool at 3.6 μmol/100 mg (dry weight) of cells (5). Also, approximately 1 mM D-amino acids are secreted from bacteria in the bacterial culture medium (20). Konno et al. observed that the D-amino acids that accumulated in urine and tissues derived from enterobacteria in $DAO^{-/-}$ mice, but not in normal mice, which indicates that DAO continuously catabolizes D-amino acids and thus generates H_2O_2 by means of endogenously derived D-amino acids in the kidney or other tissues (18). These possibilities remain to be elucidated.

These observations suggest that DAO exhibits bacteriostatic activity and bactericidal activity in the presence of MPO *in vitro*. The substrate of DAO, D-amino acids, may be supplied from infecting bacteria or endogenous bacteria *in vivo* to some extent. Thus, DAO, in combination with MPO, may be an antibacterial system in mammals, especially in the kidney but perhaps also in the lung and liver, which utilizes D-amino acids derived from endogenous bacteria in infections.

ACKNOWLEDGMENT

This work was supported by Grant-in-Aid for Scientific Research 21791016 from the Ministry of Education, Culture, Sports, Science and Technology of Japan.

REFERENCES

1. Albrich JM, McCarthy CA, Hurst JK. 1981. Biological reactivity of hypochlorous acid: implications for microbicidal mechanisms of leukocyte myeloperoxidase. Proc. Natl. Acad. Sci. U. S. A. 78:210–214.
2. Allen RC, and Stephens JT, Jr. 2011. Myeloperoxidase selectively binds and selectively kills microbes. Infect. Immun. 79:474–485.
3. Baehner RL, Nathan DG, Karnovsky ML. 1969. The metabolic and bactericidal defect in chronic granulomatous disease. Vox Sang. 17:35–36.
4. Bainton DF, Ullyot JL, Farquhar MG. 1971. The development of neutrophilic polymorphonuclear leukocytes in human bone marrow. J. Exp. Med. 134:907–934.
5. Bhattacharyya SK, Banerjee AB. 1974. D-Amino acids in the cell pool of bacteria. Folia Microbiol. 19:43–50.
6. Brenot A, King KY, Janowiak B, Griffith O, Caparon MG. 2004. Contribution of glutathione peroxidase to the virulence of Streptococcus pyogenes. Infect. Immun. 72:408–413.
7. Briggs RT, Karnovsky ML, Karnovsky MJ. 1977. Hydrogen peroxide production in chronic granulomatous disease. A cytochemical study of reduced pyridine nucleotide oxidases. J. Clin. Invest. 59:1088–1098.
8. Chumakov I, et al. 2002. Genetic and physiological data implicating the new human gene G72 and the gene for D-amino acid oxidase in schizophrenia. Proc. Natl. Acad. Sci. U. S. A. 99:13675–13680.
9. Clifford DP, Repine JE. 1982. Hydrogen peroxide mediated killing of bacteria. Mol. Cell Biochem. 49:143–149.
10. Cline MJ, Lehrer RI. 1969. D-Amino acid oxidase in leukocytes: a possible D-amino-acid-linked antimicrobial system. Proc. Natl. Acad. Sci. U. S. A. 62:756–763.
11. D'Aniello A, et al. 1993. Biological role of D-amino acid oxidase and D-aspartate oxidase. Effects of D-amino acids. J. Biol. Chem. 268:26941–26949.
12. Fang J, et al. 2008. Oxystress inducing antitumor therapeutics via tumor-targeted delivery of PEG-conjugated D-amino acid oxidase. Int. J. Cancer 122:1135–1144.
13. Fang J, Sawa T, Akaike T, Maeda H. 2002. Tumor-targeted delivery of polyethylene glycol-conjugated D-amino acid oxidase for antitumor therapy via enzymatic generation of hydrogen peroxide. Cancer Res. 62:3138–3143.
14. Haase LW. 1950. Bactericidal action of hydrogen peroxide, peroxides, and oxidizing compounds. Pharmazie 5:436–437.
15. Jaovisidha P, Peeples ME, Brees AA, Carpenter LR, Moy JN. 1999. Respiratory syncytial virus stimulates neutrophil degranulation and chemokine release. J. Immunol. 163:2816–2820.
16. Kanafani H, Martin SE. 1985. Catalase and superoxide dismutase activities in virulent and nonvirulent Staphylococcus aureus isolates. J. Clin. Microbiol. 21:607–610.
17. Klebanoff SJ, White LR. 1969. Iodination defect in the leukocytes of a patient with chronic granulomatous disease of childhood. N. Engl. J. Med. 280:460–466.
18. Konno R, Niwa A, Yasumura Y. 1990. Intestinal bacterial origin of D-alanine in urine of mutant mice lacking D-amino-acid oxidase. Biochem. J. 268:263–265.
19. Konno R, Yasumura Y. 1983. Mouse mutant deficient in D-amino acid oxidase activity. Genetics 103:277–285.
20. Lam H, et al. 2009. D-Amino acids govern stationary phase cell wall remodeling in bacteria. Science 325:1552–1555.
21. Lyle LR, Jutila JW. 1968. D-Amino acid oxidase induction in the kidneys of germ-free mice. J. Bacteriol. 96:606–608.
22. Mandell GL. 1975. Catalase, superoxide dismutase, and virulence of Staphylococcus aureus. In vitro and in vivo studies with emphasis on staphylococcal-leukocyte interaction. J. Clin. Invest. 55:561–566.
23. Nagata Y, Yamada R, Nagasaki H, Konno R, Yasumura Y. 1991. Administration of D-alanine did not cause increase of D-amino acid oxidase activity in mice. Experientia 47:835–838.
24. Paul BB, Strauss RR, Jacobs AA, Sbarra AJ. 1970. Function of H(2)O(2), myeloperoxidase, and hexose monophosphate shunt enzymes in phagocytizing cells from different species. Infect. Immun. 1:338–344.
25. Pucci MJ, Thanassi JA, Ho HT, Falk PJ, Dougherty TJ. 1995. Staphylococcus haemolyticus contains two D-glutamic acid biosynthetic activities, a glutamate racemase and a D-amino acid transaminase. J. Bacteriol. 177:336–342.
26. Robinson JM, Briggs RT, Karnovsky MJ. 1978. Localization of D-amino acid oxidase on the cell surface of human polymorphonuclear leukocytes. J. Cell Biol. 77:59–71.
27. Sakamoto R, et al. 2003. A new water-soluble chromogenic indicator: an application to the determination of chlorine in aqueous solutions. Anal. Sci. 19:1445–1447.
28. Schleifer KH. 1975. Chemical structure of the peptidoglycan, its modifiability and relation to the biological activity. Z. Immunitatsforsch. Exp. Klin. Immunol. 149:104–117.
29. Zhang H, Yang Q, Sun M, Teng M, Niu L. 2004. Hydrogen peroxide produced by two amino acid oxidases mediates antibacterial actions. J. Microbiol. 42:336–339.
30. Zhang M, et al. 2011. Behavioral characterization of a mutant mouse strain lacking D-amino acid oxidase activity. Behav. Brain Res. 217:81–87.

Current Cancer Drug Targets, 12(1), 51-63 (2012)

The Hsp32 inhibitors SMA-ZnPP and PEG-ZnPP exert major growth-inhibitory effects on $CD34^+/CD38^+$ and $CD34^+/CD38^-$ AML progenitor cells

Harald Herrmann[1,2], Michael Kneidinger[2], Sabine Cerny-Reiterer[2], Thomas Rülicke[3], Michael Willmann[4], Karoline V. Gleixner[2], Katharina Blatt[2], Gregor Hörmann[5], Barbara Peter[2,4], Puchit Samorapoompichit[6], Winfried Pickl[7], Gahininath Yadavrao Bharate[8], Matthias Mayerhofer[5], Wolfgang R. Sperr[2], Hiroshi Maeda[8], Peter Valent[1,2]*

[1]Ludwig-Boltzmann Cluster Oncology, Vienna, Austria; [2]Department of Internal Medicine I, Division of Hematology & Hemostaseology, Medical University of Vienna, Austria; [3]Institute of Laboratory Animal Science, University of Veterinary Medicine Vienna, Austria; [4]Department of Companion Animals and Horses, Clinic for Internal Medicine and Infectious Diseases, University of Veterinary Medicine Vienna, Austria; [5]Department of Laboratory Medicine, [6]Center of Anatomy and Cell Biology & [7]Institute of Immunology, Medical University of Vienna, Austria; [8]Laboratory of Microbiology and Oncology, Faculty of Pharmaceutical Sciences, Sojo University, Kumamoto and BioDynamics Research Laboratory, Kumamoto, Japan

Supported by: Austrian Federal Ministry for Science and Research (GENAU-C.h.i.l.d. grant #GZ 200.136/1-VI/1/2005), a Cancer Stem Cell grant and Initative Krebsforschung of the Medical University of Vienna; and a grant for Cancer Research from the Ministry of Education, Science, Culture, and Sports of Japan (#17016076).

Running Title: Effects of HO-1-blockers on AML cells

*Correspondence:
Peter Valent, MD
Department of Internal Medicine I
Division of Hematology & Hemostaseology
Medical University of Vienna
Ludwig Boltzmann Cluster Oncology
AKH-Wien, Währinger Gürtel 18-20
A-1097 Vienna, Austria
Phone: +43-1-40400-4416; Fax: +43-1-40400-4030
E-mail: peter.valent@meduniwien.ac.at

Abstract word count: 224 Total word count: 5,558

Key words: AML • HO-1 • Hsp32 • survival • targeting

ABSTRACT

Heat shock protein 32 (Hsp32), also known as heme oxygenase 1 (HO-1), has recently been identified as a potential target in various hematologic malignancies. We provide evidence that Hsp32 is constitutively expressed in primary leukemic cells in patients with acute myeloid leukemia (AML) and in various AML cell lines (HL60, U937, KG1). Expression of Hsp32 mRNA was demonstrable by qPCR, and expression of the Hsp32 protein by immunocytochemistry and Western blotting. The stem cell-enriched CD34+/CD38+ and CD34+/CD38- fractions of AML cells were found to express Hsp32 mRNA in excess over normal CD34+ progenitor cells. Two Hsp32-targeting drugs, pegylated zinc-protoporphyrin (PEG-ZnPP) and styrene-maleic-acid-copolymer-micelle-encapsulated ZnPP (SMA-ZnPP), were found to inhibit cytokine-dependent and spontaneous proliferation in all 3 AML cell lines as well as in primary AML cells. Growth inhibitory effects of SMA-ZnPP and PEG-ZnPP were dose-dependent with IC_{50} values ranging between 1 and 20 μM, and were accompanied by apoptosis as evidenced by light- and electron microscopy, Tunel assay, and caspase-3 activation. Finally, we were able to demonstrate that SMA-ZnPP inhibits cytokine-dependent proliferation of CD34+/CD38+ and CD34+/CD38- AML progenitor cells *in vitro* in all patients as well as leukemia-initiation of AML stem cells in NOD-SCID IL-2Rγ$^{-/-}$ (NSG) mice *in vivo*. Together, our data suggest that Hsp32 plays an important role as a survival factor in leukemic stem cells and as a potential new target in AML.

Introduction

Acute myeloid leukemia (AML) is a life-threatening neoplasm characterized by uncontrolled proliferation and accumulation of myeloblasts in hematopoietic tissues [1,2]. Clinical features and the prognosis in AML vary depending on deregulated genes, the cell type(s) involved, and the biological properties of the clone [1-4]. In a group of patients, cytogenetic features are indicative of a favorable prognosis [1,2,5]. These patients, when treated with repeated cycles of chemotherapy or hematopoietic stem cell transplantation (HSCT), have a relatively high chance to enter long-term disease-free survival [5-8]. However, not all patients have a suitable donor or are eligible for HSCT. In other patients, the response to chemotherapy is poor or short-lived. For AML patients who cannot be cured by chemotherapy or HSCT, no effective treatment alternatives are available and the prognosis is grave.

During the past few years, a number of new promising targeted drugs have been developed in clinical hematology [9-11]. A highlighting example is chronic myeloid leukemia (CML) where drugs targeting the disease-related oncoprotein, BCR/ABL, produce complete cytogenetic remission in a majority of all patients [11,12]. In AML, however, targeted drugs with comparable beneficial effects have not been developed yet. This may be due to the heterogeneity of the disease and the fact that many different oncogenes, downstream signaling pathways, and survival molecules play a role in disease evolution [3,4,9,10]. Therefore, in AML, research is currently attempting to identify not only disease-specific targets but also targets that are broadly expressed in leukemic cells in various categories of the disease [9,10,13].

One interesting group of targets in hematology are heat shock proteins (Hsp) [14-16]. These stress-related proteins act cytoprotective and anti-apoptotic in neoplastic cells in various (myeloid) leukemias [14-16]. However, so far, little is known about the expression and role of various Hsp in AML, and the effects of Hsp-targeting drugs. A particular problem is that only a few Hsp-targeting drugs are available.
Hsp32, also known as heme oxygenase-1 (HO-1), is an inducible stress-protein that acts anti-apoptotic and cytoprotective in various cells in inflammatory reactions [17,18]. More recently, it has been described that Hsp32 is also employed as a survival factor by neoplastic cells and may serve as an interesting target [19-24]. We have recently shown that leukemic cells in CML express Hsp32 in a constitutive manner, and that Hsp32 may represent a potential target in CML [25,26].
The aims of the present study were to examine the expression and functional role of Hsp32 in AML cells and to explore whether targeting of Hsp32 in leukemic (progenitor) cells is associated with apoptosis and growth arrest.

MATERIALS AND METHODS

Reagents

RPMI 1640 medium and fetal calf serum (FCS) were purchased from PAA laboratories (Pasching, Austria), hemin, cytosine arabinoside (ARA-C), and zinc-protoporphyrin (ZnPP) from Sigma-Aldrich (St. Louis, MO), and ^{3}H-thymidine from Amersham (Aylesbury, UK). Recombinant human (rh) granulocyte-macrophage colony-stimulating factor (GM-CSF) was provided by Sandoz (Vienna, Austria) and rh interleukin-3 (IL-3) by Novartis (Vienna, Austria). Rh stem cell factor (SCF) was purchased from PeproTech (Rocky Hill, NJ), and rh G-CSF from Amgen (Thousand Oaks, CA). Pegylated zinc protoporphyrin (PEG-ZnPP) and styrene maleic acid-copolymer-encapsulated zinc protoporphyrin (SMA-ZnPP) were produced at Sojo University (Kumamoto, Japan) as described [23,24,27]. The following monoclonal antibodies (mAb) were used in our flow cytometry experiments: the FITC-conjugated CD19 mAb 4G7, PE-labeled CD33 mAb WM53, PE- or FITC-conjugated CD34 mAb 581, APC-labeled CD38 mAb HIT2, and the PerCP-labeled CD45 mAb 2D1 (all from Becton Dickinson Biosciences, San Jose, CA).

Isolation of primary AML cells and culture of cell lines

Primary leukemic cells were obtained from the peripheral blood (PB) or/and bone marrow (BM) of 58 patients with either untreated AML (de novo or secondary) or relapsed/refractory AML before therapy. Diagnoses were established according to published criteria [2,28,29]. The patients´ characteristics are shown in Table 1. Detailed information on all patients including the French-American-British (FAB) cooperative study group subtype and the WHO subtype of AML are provided in supplemental Table S1. Informed consent was obtained prior to blood donation and BM puncture in each case. Mononuclear cells (MNC) were isolated using Ficoll. In a separate set of experiments, cells were preincubated with hemin (10 μM) or control medium at 37°C for 4 hours before being analyzed for Hsp32 expression [25]. In 12 patients, CD34+/CD38+ and CD34+/CD38- cells were purified to homogeneity by mAb and cell sorting on a FACSAria (Becton Dickinson Biosciences) following